Environmental Microbiology
September 2009, Volume 11, Issue 9, Pages 2446 - 2462
http://dx.doi.org/10.1111/j.1462-2920.2009.01976.x

The definitive version is available at http://www3.interscience.wiley.com/

Archaeal communities associated with shallow to deep subseafloor sediments of the New Caledonia Basin

Erwan G. Roussel[1, *, #, 3], Anne-Laure Sauvadet[1, 3], Carine Chaduteau[2], Yves Fouquet[2], Jean-Luc Charlou[2], Daniel Prieur[1], and Marie-Anne Cambon Bonavita[1]

[1] Laboratoire de Microbiologie des Environnements Extrêmes, UMR 6197, Université de Bretagne Occidentale, Ifremer, CNRS, Institut Universitaire Européen de la Mer, 29280 Plouzané, France.
[2] Département Géosciences Marines, Ifremer, Centre de Brest, 29280 Plouzané, France.
[3] Equal contribution

Present address: School of Earth and Ocean Sciences, Cardiff University, Main Building, Park Place, Cardiff, Wales, UK

*: Corresponding author : E. Roussel, Tel. (+44) 29 2087 4488; Fax (+44) 29 2087 4326, email address : RousselEG@cardiff.ac.uk

Abstract:

The distribution of the archaeal communities in deep subseafloor sediments [0–36 m below the seafloor (mbsf)] from the New Caledonia and Fairway Basins was investigated using DNA- and RNA-derived 16S rRNA clone libraries, functional genes and denaturing gradient gel electrophoresis (DGGE). A new method, Co-Migration DGGE (CM-DGGE), was developed to access selectively the active archaeal diversity. Prokaryotic cell abundances at the open-ocean sites were on average 3.5 times lower than at a site under terrestrial influence. The sediment surface archaeal community (0–1.5 mbsf) was characterized by active Marine Group 1 (MG-1) Archaea that co-occurred with ammonia monooxygenase gene (amoA) sequences affiliated to a group of uncultured sedimentary Crenarchaeota. However, the anoxic subsurface methane-poor sediments (below 1.5 mbsf) were dominated by less active archaeal communities, such as the Thermoplasmatales, Marine Benthic Group D and other lineages probably involved in the methane cycle (Methanosarcinales, ANME-2 and DSAG/MBG-B). Moreover, the archaeal diversity of some sediment layers was restricted to only one lineage (Uncultured Euryarchaeota, DHVE6, MBG-B, MG-1 and SAGMEG). Sequences forming two clusters within the Thermococcales order were also present in these cold subseafloor sediments, suggesting that these uncultured putative thermophilic archaeal communities might have originated from a different environment. This study shows a transition between surface and subsurface sediment archaeal communities.

Introduction

The sub-seafloor biosphere may comprise as much as two thirds of Earth's total prokaryotic biomass (Whitman et al., 1998) and extends to at least 1626 meters below the seafloor (mbsf) (Roussel et al., 2008). Ubiquitous microbial communities present in the sub-seafloor play an important role in global biochemical cycles (e.g. D'Hondt et al., 2004). The prokaryotic cell density drastically decreases with depth and decreasing available energy supply due to reduction in efficient electron acceptors and bioavailable organic carbon sources (Parkes et al., 2000; Schippers et al., 2005). However, local increases in cell density occur in response to specific geochemical and lithological conditions (D'Hondt et al., 2004; Parkes et al., 2005; Sørensen and Teske, 2006).

The boundary between surface and subsurface could be defined as a change of the microbial community composition, shifting from surface (e.g. the water column) to deep subsurface communities (Teske and Sørensen, 2008). Moreover, microbial metabolic processes in marine sediments are generally stratified according to the sequential consumption of electron acceptors diffusing into sediments from the overlying seawater. Oxygen, the main electron acceptor in surface sediment, is rapidly depleted, followed by nitrate and manganese (Froelich et al., 1979). However, in deeper anoxic sediments, sulfate reduction and methanogenesis may represent the main metabolic processes in the deep sub-seafloor (D'Hondt et al., 2002; D'Hondt et al., 2004; Parkes et al., 2005). Organic rich coastal sediments, under terrestrial influence, harbor higher microbial densities and activities compared to open-ocean sediments (D'Hondt et al., 2004). Hence, there appears to be a correlation between the origin of the organic matter and biochemical processes, such as methanogenesis (Sivan et al., 2007). Active archaeal communities, involved in biochemical cycles such as methane cycling at depth, could represent a significant fraction of the microbial community of the deep marine subsurface (Biddle et al., 2006; Sørensen and Teske, 2006; Lipp et al., 2008).

The distribution and metabolisms of the sub-seafloor microbial communities are mostly understood through culture-independent techniques (e.g. Newberry et al., 2004; Parkes et al., 2005; Biddle et al., 2006; Fry et al., 2006; Sørensen and Teske, 2006; Biddle et al., 2008), since most of these prokaryotes do not have a closely related cultured relative. In shallow marine sediments, DNA-based molecular approaches are strongly biased as up to 90% of the total DNA is extra cellular (Danovaro et al., 1999; Dell'Anno and Danovaro, 2005), resulting in an inability to distinguish between living and dead microbial communities (Dell'Anno and Corinaldesi, 2004; Damste and Coolen, 2006). In order to target metabolically active communities, to correlate their phylogeny with variable environmental factors, fluorescent in situ hybridization has commonly been used (e.g. Treude et al., 2005; Biddle et al., 2006). However this approach does not provide an overall picture of the active microbial communities. As rRNA has a rapid turnover (Kemp et al., 1993; Kerkhof and Ward, 1993; Kramer and Singleton, 1993; Danovaro et al., 1999), extractable archaeal rRNA can be used to target the active cells from subsurface sediments (Lloyd et al., 2006; Sørensen and Teske, 2006; Roussel et al., 2009).

The current study investigates some of the spatial and abiotic variables that could possibly control the archaeal community distribution and activities in deep-sea sediments. The analysis of the archaeal diversity and community structures was performed on surface and subsurface sediments from the New-Caledonia and Fairway Basins, with different terrestrial influences, using denaturant gradient gel electrophoresis (DGGE) and cloning PCR-amplified phylogenetic and functional genes. The active fraction of the archaeal community in deep-sea sediments was also assessed by a new molecular approach based on DGGE.

Results and discussion

Site description and total prokaryotic count depth profiles

The sediment samples were collected from six sites in the New Caledonia and Fairway basins during the Oceanographic cruise ZoNéCo 12 in February 2006 (Fig. 1). Site MD06-3019 sediments, located in a canyon deriving a substantial amount of terrigenous matter from New Caledonia, comprised a succession of terrigenous sequences composed of dark carbonate clay interspaced with sands (Foucher et al., 2006). Moreover, MD06-3019 sediments had higher contents of minerals from a probable detrital origin such as quartz, chlorite, kaolinite, montmorillonnite, halite and albite, than MD06-3018 sediments, which displayed higher contents of calcite (data not shown). In contrast with site MD06-3019, site MD06-3018 sediments were situated in an open-ocean context, characterized by homogeneous sediment facies composed of foraminiferal clay (Foucher et al., 2006). In the Fairway Basin, sites MD06-3022, MD06-3026, MD06-3027 and MD06-3028 sediments were also located in an open-ocean context. Site MD06-3027 represented a reference zone, in contrast with MD06-3022 and MD06-3028 where the sedimentary sequence was pierced by a diapir (see *supplementary material*, Fig. S1) and showed an extensive faulting in the sedimentary cover which could be the consequence of gas migration through the sediment cover (Auzende et al., 2000).

On the whole, the prokaryotic cell counts were within the limits of the general depth distribution model (Parkes et al., 2000), although the distribution at site MD06-3019 was more heterogeneous than at the open-ocean sites, fluctuating between the lowest and highest prediction limits (Fig. 2). Moreover, the low cell number, between 7.5 mbsf and 10.5 mbsf at site MD06-3019, was correlated with the occurrence of driftwood in the sediment. Therefore, as the core lithology comprised a succession of terrigenous sequences, the heterogeneous prokaryotic cell number distribution and methane depth profile might be related to the strong erosion events of New Caledonia. Although the prokaryotic abundances at the open-ocean sites (MD06-3022, MD06-3026 and MD06-3028) were ~3.5 times lower than at the site under terrestrial influence (MD06-3019), no correlation was found between prokaryotic counts and biogeochemical data (Fig. 2). However the low cell numbers and methane content in the Fairway Basin sediments are consistent with the general depth distribution of methane and prokaryotic cells in open-ocean sub-seafloor sediments, presumably reflecting the lower inputs of organic carbon compared with the site under terrigenous influence (Wellsbury et al., 2002; D'Hondt et al., 2004).

Archaeal community structure

Co-Migration DGGE (CM-DGGE). One of the most revealing questions, in sub-seafloor studies, is discriminating and identifying active and living from the dead or quiescent microbial communities. Nucleic acid-based molecular analyses of deep sub-seafloor microbial communities are limited, as sediment samples are usually characterized by low biomass, limited material and the presence of PCR inhibitors (Webster et al., 2003). Fingerprinting techniques, such as DGGE, are recommended for describing the microbial community structures, as a large number of samples can be analyzed (for review, see Smalla et al., 2007). However, as DGGE analyses can be biased by gel variations (e.g.

Ferrari and Hollibaugh, 1999; Nunan et al., 2005), running intra-lane standards enhances sample-to-sample comparisons (Muyzer, 1999; Neufeld and Mohn, 2005). Here, we developed a new fingerprinting approach based on DGGE and named Co-Migration DGGE (CM-DGGE, see *experimental procedures*), adapting the use of different terminally labelled fluorescent PCR products, to compare simultaneously the DNA- and RNA-derived microbial community in deep-sea sediments. As the use of labelled primers improves the sensitivity and specificity of DGGE fingerprint detection (Neufeld and Mohn, 2005), it is possible to use rRNA to detect minor archaeal activities, such as the *Thermococcales Group 1* (TG-1) at site MD06-3019 (see *supplementary material*, Fig. S6). Moreover, this technique is also time saving and minimizes the problems of gel handling and staining.

***Cluster analysis of DGGE profiles*.** All the DNA-derived 16S rRNA PCR products from all depths were screened by DGGE prior cloning, in order to select the depths with the most representative archaeal phylogenetic distribution for each core (Webster et al., 2003), and to assess the archaeal community structures. As the degree of separation between DGGE fragments decreases with size due to the melting of multiple melting domains in the larger fragments (Myers, 1988; Sheffield et al., 1989), two sets of primers ($A344f^{GC}$-A915r and Saf-PARCH 519r) and gel conditions were optimized in order to obtain different scales of band discrimination (Roussel et al., unpublished data). However, the PCR surveys of archaeal communities using the Saf-PARCH 519r primer set were probably less biased than with $A344f^{GC}$-A915r primer set, as there is a lower number of primer mismatches with specific subsurface and hydrothermal vent archaeal sequences (Teske and Sørensen, 2008). The resulting dendrogram of DGGE patterns, using Saf-PARCH 519r, displayed two major clusters (see *supplementary material*, Fig. S2C). The Cluster A depths ranged from 0 to 1.5 mbsf, except for two samples (7.5 and 9 mbsf) and had fragments exclusively affiliated to MG-1, whereas cluster B was composed of fragments related to 6 different phylotypes (Fig. S2B, Rice cluster V, *Thermoplasmatales*, MBG-D, SAGMEG, unclassified *Euryarchaeota*).

***Statistical analyses of the clone libraries*.** According to the results of the DGGE screening, twenty five different clone libraries were constructed, representing a total of 771 sequences

(Fig. 3). Whole 16S rRNA sequences, derived from RNA and DNA, were assigned to 71 OTUs based on a 95% genus level of phylotype differentiation (Schloss and Handelsman, 2004). Amplifiable DNA was obtained from all depths, and 1 to 13 OTUs were respectively assigned per clone library. The DNA-derived clone libraries were named DNAxTy, where "x" represents the core number and "y" the depth in centimetres of the clone library (Fig. 3). Amplifiable RNA was only obtained above 1.5 mbsf and was not detected at any other depth (Fig. 5 and S6). Thus, two RNA-derived clone libraries, named RNA18T150 (MD06-3018, 1.5 mbsf) and RNA19T150 (MD06-3019, 1.5 mbsf), were respectively assigned with 27 OTUs and 5 OTUs. The coverage values for the 16S rRNA gene clone libraries ranged from 18 to 100% (Fig. 3). Rarefaction curves were strongly curvilinear for all clone libraries attesting adequate sampling, except for DNA19T150 and DNA19T4 as a result of strong intra-lineage diversities (see *supplementary material*, Fig. S3).

The archaeal diversity of the seawater clone library (Fig. 3) was significantly different from all sediment clone libraries ($P < 0.01$), suggesting that the detected *Archaea* are marine sediment communities. Moreover, differences between all DNA-derived clone library diversity indices (F_{ST} and the exact test method) were statistically significant ($P < 0.01$) except between 13 clone libraries distributed among three groups, as described in figure 3. The clone libraries of each group were from similar lineage distributions and matched the cluster analysis of DGGE band patterns, except for DNA28T450 (Fig. 3 and S2). Both the cluster analysis of DGGE band patterns and the distribution of archaeal lineages in clone libraries showed distinct phylogenetical archaeal communities (except for the MG-1 lineage) either restricted to surface (0 to 1.5 mbsf) or to subsurface (below 1.5 mbsf) sediment horizon (Fig. 3 and S2) suggesting that these archaeal communities could be adapted to specific sedimentary environmental conditions.

Archaeal diversity and metabolic activity: from the sediment surface to the subsurface

Sediment surface. The sediment surface archaeal communities of all clone libraries and DGGE community structures above 1.5 mbsf were exclusively dominated by crenarchaeal phylotypes related to Marine Group I (MG-1; Fig. 3 and S2). The MG-1 diversity was high (Fig. 4), covering more than five subclades (α, β, ε, ξ and η) and only related to sequences from deep marine sediments (Newberry et al., 2004; Sørensen et al., 2004; Teske and Sørensen, 2008). MG-1 *Archaea*, identified as aerobic autotrophic ammonia oxidizers (Francis et al., 2005; Könneke et al., 2005; Hallam et al., 2006), are commonly found in seawater and marine sediments, forming several phylogenetic clusters with currently two cultured relatives (Preston et al., 1996; Könneke et al., 2005). Moreover, based on the analysis of the first sequenced genome of a cultured relative (*Crenarchaeum symbiosum*), the MG-1 were recently proposed as a novel archaeal phylum named *Thaumarchaeota* (Brochier-Armanet et al., 2008). The seawater archaeal diversity, in the CTDII clone library, was exclusively composed of sequences related to marine groups, such as MG-1 (95%), MG-2 (3%) and MG-3 (2%) (Fig. 3). However, only two sequences (DNA19T150), out of 673 rRNA gene sequences from sediment samples, matched with sequences from the seawater clone library (Fig. 4), and *amoA* genes related to seawater phylotypes were not detected (Fig. 6), which suggests that contamination of the sediment by seawater was negligible. As the MG-1 phylotypes retrieved in the sediments were different from those found in the oxic seawater, specific MG-1 subclades could be adapted to sedimentary suboxic conditions (Teske and Sørensen, 2008).

The active fraction of the archaeal community was assessed by Co-Migration DGGE (CM-DGGE) analysis of reverse-transcribed and PCR-amplified rRNA and compared to the DNA-derived archaeal community. By using the same primer sets and gel conditions as for the previous DGGE analyses, we showed that the archaeal communities were most active between 0 to 1.5 mbsf, as no rRNA was detected below 1.5 mbsf (Fig. 5 and S6), and that they were composed of MG-1 *Archaea*. Congruently, the two RNA-derived libraries (RNA18T150 and RNA19T150) were dominated by sequences related to the same MG-1 sequences as the DNA-derived libraries (Fig. 4) demonstrating that these sediment surface MG-1 communities were active. Moreover, insignificant F_{ST} and P tests ($P < 0.01$) suggested that the sequences from the DNA19T0, DNA19T2, DNA19T4, RNA18T150 and RNA19T150 clone libraries were from similar lineage distributions and were indistinguishable from the combined communities. However, although the molecular techniques (reverse transcription, PCR and cloning), used to build clone libraries, are known to be inherently biased (Suzuki and Giovannoni, 1996; von Wintzingerode et al., 1997), significant differences in lineage distribution were detected between the RNA and DNA derived libraries at the same depth (RNA18T150, RNA19T150, DNA18T150 and DNA19T150). The ratios between the 16S rRNA gene and 16S rRNA per cell have been reported to be proportional to the metabolic activity of the cells (Dell'Anno et al., 1998), the rRNA content per cell increasing with metabolic activity. As the MG-1 lineage was detected in RNA18T150 and RNA19T150 libraries, whereas absent in DNA18T150 and DNA19T150 libraries, we suggest that the sediments at 1.5 mbsf could have low cell concentrations of very active MG-1 lineage.

As MG-1 are putative ammonia-oxidizing *Archaea*, amplifications of the *amoA* gene, using archaeal *amoA* primers (Francis et al., 2005), were performed in order to confirm the occurrence of ammonia-oxidizing *Archaea* (AOA) in deep marine sediments at sites MD06-3018 and 3019. Archaeal *amoA* gene was only detected between the sediment surface and 1.5 mbsf. Moreover, to investigate the *amoA* gene diversity, two archaeal *amoA* libraries (n = 40, coverage = 83%) were analyzed. These libraries were exclusively composed of 635-bp length sequences related to uncultured *Crenarchaeota* (Fig. 6). These sequences formed 15 OTUs (based on a 2% cut-off) grouping in a distinct phylogenetic group of sequences from sediments (Francis et al., 2005). However, no *amoA* sequences related to water column *Archaea* were detected (Francis et al., 2005) (Fig. 6), suggesting that *amoA* sequences retrieved were from archaeal communities adapted to sedimentary environments. Moreover, *amoA* genes related to the sediment cluster were only retrieved at the depths where MG-1 rRNA genes were detected. Altogether, these evidences suggest that ammonia-oxidizing could be one of the main archaeal activities at the sediment surface.

Subseafloor MG-1 *Archaea* were also detected at some sites below 1.5 mbsf characterized by an extensive faulting in the sedimentary cover (MD-3026 and 3028; Fig. 3). These sub-surface MG-1 communities were phylogenetically related to the MG-1 *Archaea* found at the sediment surface horizon, and *amoA* genes related to MG-1 were only detected at depths containing MG-1 rRNA genes. Therefore, these communities might be fuelled by ammonium rich fluids originating either from seawater intrusion or from fluid advection from depth. However, no RNA was detected from these depths, suggesting that sub-surface MG-1 are less active or less abundant than the surface communities.

Sediment subsurface. The sub-surface archaeal community, restricted to depths below 1.5 mbsf, was composed of typical sub-seafloor lineages (Fig. 3, S4 and S5, MBG-B, MBG-D, MCG and SAGMEG; for review, see Teske and Sørensen, 2008) usually detected in subsurface sediments and methane-rich environments (Bidle et al., 1999; Inagaki et al., 2003; Newberry et al., 2004; Sørensen et al., 2004; Parkes et al., 2005; Inagaki et al., 2006b; Sørensen and Teske, 2006). A majority of sequences were related to uncultured environmental sequences from these environments (Fig. S4 and S5, highest similarity to pure culture, 99%). The sediment-derived clone library diversities were very heterogeneous, either strongly dominated by sequences related to *Euryarchaeota* or by sequences related to *Crenarchaeota* (Fig. 3). Overall, euryarchaeal lineages represented less than 1% of the clone libraries from surface sediments (0 to 1.5 mbsf), whereas below they represented 59% (Fig. 3). The whole *Euryarchaeota* phylogenetic diversity was high, representing a total of 10 different lineages (Fig. 3 and S4): *Methanococcoides,* Novel *Methanosarcinales* group 1 (NMG-1)*, Methanosaeta,* ANME-2, *Thermoplasmatales*, Marine Benthic Group D (MBG-D), Deep-Sea Hydrothermal Vent Euryarchaeotal Group 6 (DHVE6), South African Gold Mine Euryarchaeotic Group (SAGMEG), *Thermococcales* and Uncultured *Euryarchaeota* (for review see Teske and Sørensen, 2008). Sequences related to the very ubiquitous *Thermoplasmatales* and MBG-D lineages were found in 44% of the libraries, representing 26% of the clones in the libraries below 1.5 mbsf (Fig. 3), suggesting that these lineages could be shallow sediment subsurface-dwelling *Archaea* (for review see Teske and Sørensen, 2008). The crenarchaeal sequences, detected below 1.5 mbsf, clustered into the Miscellaneous Crenarchaeotic Group (MCG) (<1%) and the Marine Benthic Group B (MBG-B, also called DSAG) lineages (15%) (Fig. 3, Fig. S2 and S5). MCG *Archaea* are very ubiquitous in sediment subsurface environments and are thought to be heterotrophic anaerobes utilizing complex organic substrates (Teske and Sørensen, 2008; Fry et al, 2008). Although the small number of sequences related to MCG *Archaea* retrieved from the New Caledonia and Fairway Basins sediments could be the result of the low organic matter concentrations of these sediments, it is more likely to be the consequence of a primer-related bias, as the primer A344f contains a high number of mismatches with most of the known MCG 16S rRNA genes (Teske and Sørensen, 2008). The archaeal diversity of some sediment layers at different sites was restricted to only one lineage (Fig. 3, Uncultured *Euryarchaeota*, DHVE6, MBG-B, MG-1 and SAGMEG). Moreover, uncultured *Euryarchaeota*, DHVE6 and SAGMEG were not detected in any other sediment samples, suggesting that these *Archaea* may have been selected by specific environmental conditions. However, no archaeal rRNA was retrieved below 1.5 mbsf, presumably being below the detection limit (Fig. S6), suggesting that these probably less active deep subseafloor archaeal communities are adapted to these low energy and organic carbon availability environments (D'Hondt et al., 2002; Valentine, 2007).

Sulfate reduction and methane cycling activities widely occur in deep marine sediments (D'Hondt et al., 2002; D'Hondt et al., 2004; Parkes et al., 2005; Biddle et al., 2006; Sørensen and Teske, 2006; Webster et al., 2008). At site MD06-3019, sodium ($r = 0.919$; $P < 0.0001$) and chloride ($r = 0.774$; $P < 0.0001$) concentrations increased, whereas sulfate ($r = -0.913$; $P < 0.0001$) and calcium ($r = -0.931$; $P < 0.0001$) concentrations decreased with increasing depth (Fig. 2). Although sulfate concentrations decreased with increasing depth at all sites, suggesting the occurrence of sulfate-reducing prokaryotes, no genes encoding for the dissimilatory sulfate reductase (*dsr*) were detected (data not shown), probably resulting from a too low number of sulfate-reducing bacteria. Methane was the only volatile hydrocarbon detected from all sites and co-occurred with relatively high concentration of sulphate (Fig. 2). Though concentrations at all sites were very low, the increase in methane concentrations at sites MD06-3022 ($r = 0.996$; $P < 0.001$), MD06-3026 ($r = 0.881$; $P < 0.05$) and MD06-3028 (r

$= 0.999$; $P < 0.0001$) was correlated with increasing depth (Fig. 2), suggesting the occurrence of methanogenesis. Remarkably, although 16S rRNA gene sequences related to methanogenic and methanotrophic *Archaea* are very rarely detected in deep sub-seafloor sediments (Parkes et al., 2005), putative methane cycling communities represented almost 4% of the libraries below 1.5 mbsf (Fig. 3). A large proportion of these sequences (44%) were related to the *Methanococcoides* lineage, a methylotrophic methanogen (Singh et al., 2005). The methanogens utilizing C1 compounds usually dominate the marine methanogens within the zone of sulfate reduction, since sulfate reducing bacteria (SRB) do not compete for the same substrates (Purdy et al., 2003). Moreover, two sequences related to Novel *Methanosarcinales* group 1 (NMG-1), a new uncultured phylotype in the *Methanosarcinaceae* family (Roussel et al., 2009) (see *supplementary material*, Fig. S4), were retrieved from open-ocean sites (DNA19T150 and DNA22T150). These sequences grouped with environmental clones (highest similarity to pure culture, 96% to *Methanolobus oregonensis)* from a sulfide rich spring (Elshahed et al., 2004) and from estuary sediments (Purdy et al., 2002; Roussel et al., 2009). Interestingly, although *Methanosaeta Archaea* are acetoclastic methanogens that can be out-competed by SRBs in the sulfate reduction zone (for review, see Muyzer and Stams, 2008), 16S rRNA sequences related to this putative methanogenic lineage were detected in sulfate rich sediments at the open-ocean sites (Fig. 3 and S4). Theoretically competitive prokaryotic activities, such as sulfate reduction and methanogenesis, seem to co-occur at the same sediment horizons in several other deeper subseafloor sediments (D'Hondt et al., 2004; Parkes et al., 2005; Webster et al., 2008), suggesting that the in-situ environmental conditions may strongly modify the interactions between these metabolic pathways (D'Hondt et al., 2004; Webster et al., 2008). Moreover, two sequences related to ANME-2 *Archaea*, a putative anaerobic methane oxidizer that is usually found in association with SRBs (Hinrichs et al., 1999; Boetius et al., 2000) and rarely detected in deeper subsurface sediments (Roussel et al., 2008), were detected (Fig. 3 and S4), suggesting that methane and sulphate concentrations in these open-ocean sediments might be sufficient to enable a detectable ANME biomass to develop. Moreover, MBG-B

Archaea, a lineage that may possibly benefit directly or indirectly from anaerobic methane oxidization (AOM) (Biddle et al., 2006; Sørensen and Teske, 2006; Teske and Sørensen, 2008), are numerous in clone libraries below 1.5 mbsf (15%). The MBG-B *Archaea* are limited to marine environments such as hydrothermal vents (Takai and Horikoshi, 1999), cold seeps (Lloyd et al., 2006) and subsurface sediments (Biddle et al., 2006; Sørensen and Teske, 2006). However, although no methyl-coenzyme M reductase (*mcr*) genes were retrieved (data not shown), the detection of putative methanotrophs, acetoclastic methanogens and methylotrophic methanogens at two open-ocean sites, suggests that low methane cycling rates may comprise a proportion of the archaeal activities at these sites.

Contamination by exogenous DNA was of particular concern (see *Experimental Procedures*), and as all contamination controls were negative, the detection of rarely detected sub-seafloor sediment lineages, such as *Methanosarcinales* and *Thermococcales* (Fig. 3), was probably related to methodological implications. The 16S rRNA gene PCR-based surveys are biased, as only the most abundant lineages with very similar matching priming sites are detected (Teske and Sørensen, 2008). Thus, the several DNA extractions followed by pooling and concentration of several PCR and nested PCR products (increasing sensitivity), combined to the use of a primer (A344f) containing degeneracies (Teske and Sørensen, 2008), may reduce stochastic PCR biases and facilitate the detection of these rare deep sub-seafloor lineages.

***Thermococcales*.** Although sites MD06-3018 and MD06-3019 were geographically close (< 100 km), they showed drastic differences in lithology and archaeal diversity. The MD06-3018 sediments were mainly characterized by a homogeneous distribution of carbonate clay and a high diversity of archaeal lineages commonly found in marine sediments, in contrast with the MD06-3019 sediments which were characterized by a heterogeneous distribution of sand and clay and a very specific archaeal diversity. Although the *in-situ* sediment temperatures at all sites were in a range between 2 to 3°C (Foucher et al., 2006), the low archaeal diversity, retrieved from the DGGE and clone library analysis of MD06-3019 sediments below 1.5 mbsf (Fig 3, S2), was exclusively dominated by *Thermococcales*, a putative (hyper) thermophilic

Euryarchaeota commonly found at hydrothermal vent sites and representing an excellent indicator of subseafloor ecosystems (Kelley et al., 2002). These sequences were shown to form a unique cluster (Fig. 7), named *Thermococcales Group 1* (TG-1), within the genera *Thermococcus.* TG-1 16S rRNA gene sequences contain a high GC content (66%), and were related to sequences retrieved from sulphide rich hydrothermal environments (Summit and Baross, 2001). Sequences affiliated to putative *Thermococcales* have been previously detected in other cold (1-12°C) deep marine sediments (Inagaki et al., 2001; Kormas et al., 2003; Inagaki et al., 2006a). Their occurrence was usually interpreted as a deposition resulting from fluid migration, or as buried microbial relicts, representing “fossil DNA” (Inagaki et al., 2001; Kormas et al., 2003; Inagaki et al., 2006a). Even though the minimum temperature required for the growth of a *Thermococcus* is 40°C (Miroshnichenko et al., 2001), *Thermococcales* can survive over long periods in cold (4°C), oxygenated samples (Jannasch et al., 1992), possibly allowing a wide dissemination in marine environments. Interestingly, a reverse-transcribed and PCR-amplified rRNA fragment related to the *Thermococcales* order was detected from site MD06-3019 at 0.6 mbsf by CM-DGGE and was correlated with the occurrence of an authigenic mineral (aragonite), indicating the presence of probably viable *Thermococcales* at this depth (see *supplementary material*, Fig. S6). All the sequences affiliated to the *Thermococcales* order found at MD06-3019 grouped in a unique cluster (TG-1), therefore suggesting an identical origin (Fig. 7). Recently, an extensive active alkaline hydrothermal field was revealed in the south-west lagoon of New Caledonia (Pelletier et al., 2006). As the MD06-3019 site shows no signs of fluid migration and as it is located in a canyon deriving substantial amounts of terrigenous matter from the lagoon, we suggest that the TG-1 could have rafted from New-Caledonia on biotic or terrigenous substrates (Thiel and Gutow, 2005; Thiel and Haye, 2006), progressively becoming less active as organic matter became recalcitrant with burial (Wellsbury et al., 2002).

A distinct *Thermococcus* cluster was detected at site MD06-3028, grouping with sequences retrieved from deep hot subseafloor sediments (Roussel et al., 2008); for that reason, it was named *Deep Sub-Seafloor Thermococcales Group* (DSSTG). Yet, the *Thermococcales* detected were characterized by a probably low activity as no rRNA phylotypes were detected by RT-PCR. However, the DSSTG *Archaea* were only detected at this strongly faulted open-ocean site (MD06-3028, Fig. S1), whereas absent at the non-faulted adjacent reference site MD06-3027, suggesting that these communities could have been introduced by a vertical fluid migration.

In conclusion, the deep marine sediment archaeal distribution clearly differs from the seawater and depends on spatial and geochemical variables as previously shown (Parkes et al., 2005; Fry et al., 2006; Sørensen and Teske, 2006). This study also shows the transition between active surface archaeal communities, a component of which is probably capable of ammonium oxidation and less active deep typical sub-seafloor lineages possibly related to the methane cycle. Moreover, the occurrence of putative thermophiles in cold marine sediments suggests a possible dispersion of these typical hydrothermal archaeal communities.

Experimental Procedures

Site description and sampling

Six piston cores (MD06-3018, MD06-3019, MD06-3022, MD06-3026, MD06-3027, and MD06-3028) were collected from the New Caledonia and Fairway basins (Fig. 1) during *Marion Dufresne* Cruise ZoNéCo 12 in 2006, using a Calypso piston corer. Site MD06-3018 (23°00.19'S, 166°08.97'E; 2470 meters water depth; core length 24.96 m), located on the New Caledonian Basin 50 km off the New Caledonia coast, is mainly in an open-ocean context (Foucher et al., 2006). Site MD06-3019 (22°30.64'S, 165°11.75'E; 3522 meters water depth; core length 36.25 m), 80 km off the coast, is located in a canyon deriving a substantial amount of terrigenous matter (Foucher et al., 2006). Sites MD06-3022 (23°12.11'S, 163°27.94'E; 2294 meters water depth; core length 8.43 m), MD06-3026 (23°56.26'S, 163°27.72'E; 2717 meters water depth; core length 9.40 m), MD06-3027 (24°40.61'S, 163°36.14'E; 2720 meters water depth; core length 5.22 m), and MD06-3028 (24°45.20'S, 163°36.95'E; 2716 meters water depth; core length 8.03 m) are located in an open-ocean context in the Fairway Basin.

The cores were aseptically sub-sampled on board, every 20 cm on the first 100 cm, and then every 150 cm, using 5 mL syringes (luer end removed). The samples were then immediately stored anaerobically at –80°C for molecular analysis and at 4°C for prokaryotic enumeration and for enrichment cultures.

As a contamination control, seawater from the water column was collected (MD06-CTD2; 24°45.22'S, 163°36.95'E, 2690 meters water depth) using a CTD rosette and immediately stored at –80°C.

Total prokaryotic cell enumeration

Total prokaryotic counts were determined, with an epifluorescence microscope (BX60, Olympus™), by acridine orange staining, on subsamples stored at 4°C under anaerobic conditions in the dark (< 5 days), as previously described (Cragg et al., 2000).

Mineralogical composition of sediments

The mineralogy of 8 sediment samples from cores MD06-3018 and MD06-3019 was determined by X-ray diffraction (XRD) analysis using a Bruker D8 Advance equipped with a Cu X Ray tube and a Vantec detector. Samples were not dried before analysis and diffraction patterns were obtained between 5 and 70 degrees. Mineral determination and semi-quantitative estimations were performed with the EUA program.

Geochemical analysis

Methane analyses were performed on cores MD06-3019, MD06-3022, MD06-3026, MD06-3027 and MD06-3028, at the end of each core segment (1.5 m long), using the headspace technique. The cores were immediately sub-sampled on board using 5 mL syringes (luer end removed) and added to headspace vials (20 mL) filled with a NaCl/$HgCl_2$ work solution. Methane concentrations were determined using a HP 7694 automatic headspace sampler connected to a HP 5890 gas chromatograph equipped with FID and TCD detectors. The 2-

sigma uncertainty is better than 4% (Donval et al., unpublished). Results are expressed as microlitre per litre of sediment (µL/L).

Pore-waters were extracted on board from MD06-3019 and MD06-3022 cores from the end of each core segment by centrifuging sediment samples (10000 rpm over 30 min). The dissolved anions (SO_4^{2-}, Cl^-) and cations (Na^+, Ca^{2+}, Mg^{2+}) were determined from diluted pore-waters using a Dionex DX100 ion chromatograph. The IAPSO standard seawater was used for calibration and quality control. Results are expressed as millimole per litre pore-water (mM).

DNA extractions and PCR amplification

To avoid contaminations, all manipulations were carried out in a PCR cabinet exclusively dedicated to the present study (Biocap™ RNA/DNA, erlab®), using Biopur® 1.5 mL Safe-Lock micro test tubes (Eppendorf™), Rnase/Dnase Free Water (MP Biomedicals™) and UV-treated (>60 min) plasticware and pipettes.

DNA was extracted, pooled and purified from 5 × 1g uncontaminated frozen sample following a modified FastDNA® Spin Kit for Soil (Bio101 Systems, MP Biomedicals™) protocol (Webster et al., 2003; Roussel et al., 2009).

All amplifications were performed using a "GeneAmp PCR system" 9700® (Applied Biosystems™). All PCR mixtures (50 µL) contained 5 µL of DNA template, 1X Taq DNA polymerase buffer (MP Biomedicals™), 1 µL of dNTP (10 mM of each dATP, dCTP, dGTP and dTTP), 10 µM of each primer and 0.5 µL of Taq DNA polymerase (MP Biomedicals™). Negative controls were also carried out with DNA extractions performed with no sample. For all controls, no PCR products were detected.

Archaeal 16S rRNA gene amplification was conducted by nested PCR with combination of primers A8f (5'-CGG TTG ATC CTG CCG GA-3') and A1492r (5'-GGC TAC CTT GTT ACG ACT T-3') in the first round (Teske et al., 2002; Lepage et al., 2004), and with A344f (5'-AYG GGG YGC ASC AGG SG-3') and A915r (5'-GTG CTC CCC CGC CAA TTC CT-3') in the second round (Stahl and Amann, 1991; Sørensen et al., 2004). PCR cycles for the first round

(A8f/A1492r), and for the second round (A344f/A915r) were as previously described (Roussel et al., 2009). To minimize stochastic PCR bias, five independent PCR products from the first round were pooled and purified (QIAquick PCR purification Kit; Qiagen™) and used as template for the second round. This nested PCR was necessary to obtain visible PCR products on a 0.8% (w/v) agarose gel stained with ethidium bromide.

A portion of the *amoA* gene (635 bp) was amplified with primers Arch-amoAF and Arch-amoAR (Francis et al., 2005), and the following reaction conditions were performed: 1 cycle of 5 min at 95°C, 35 cycles of 45s at 94°C, 60s at 53°C and 60s at 72°C, and 1 cycle of 15 min at 72°C.

RNA extractions and RT-PCR amplification

Total RNA was extracted from each uncontaminated frozen sample (5 × 1g) using the FastRNA® Pro soil direct Kit (Bio101 Systems, MP Biomedicals™) as previously described (Roussel et al., 2009), with the following modifications: the addition of 170 µg poly-adenylic acid, tubes kept on ice and extended spin. After bead-beating on a FastPrep FP120 homogenizer (Bio101 Systems, MP Biomedicals™), the ¾ of the aqueous phases were transferred to a new tube before the remaining aqueous phases were homogenized a second time. After the addition of 660 µL of isopropanol (100%), the tubes were incubated 60 min at –20°C followed by centrifugation at 20000 × g for 15 min at 1°C. In order to increase the RNA yield, the extraction procedure was ended after the first ethanol wash and diluted in 100 µL of DEPC water.

To digest trace amounts of DNA, the extraction products were immediately pooled and 150 µL were incubated 1 hour at 37°C with 1X of TURBO DNase® buffer and 18U of TURBO DNase® (Ambion™). The digestion was stopped by adding EDTA to a final concentration of 15 mM and heating 10 min at 65°C. The product was finally concentrated and purified with the RNeasy minikit (Qiagen™), following manufacturer's instructions, to give a final volume of 100 µL.

The purified RNA product was immediately serially diluted (1 to 50 times) and reverse transcribed using the OneStep RT-PCR kit (Qiagen™), according to the manufacturer's instructions, with combination of 16S rRNA primers for *Archaea* with A8f-A1492r and the following touchdown PCR protocol as previously described (Roussel et al., 2009). To obtain visible products, a nested PCR was performed as described for the 16S rRNA gene amplification. Nested PCR assays, using the 16S rRNA primers for *Archaea*, without the reverse transcribed step, showed no DNA contamination.

DGGE analysis

In order to obtain the general archaeal 16S rRNA gene depth diversity, a PCR-DGGE analysis was performed. To avoid background interference, visualization of unspecific fragments, and to increase sensitivity and resolution, nested PCR was performed as described for the archaeal 16S rRNA gene amplification using a Cy3 labelled reverse primer Saf-PARCH 519r*Cy3 or $A344f^{GC}$-A915r*Cy3. All manipulations were performed in the dark. The touchdown PCR protocol was as previously described (Casamayor et al., 2000; Nicol et al., 2003). The PCR products were analyzed by DGGE using a DCode Universal Mutation Detection System® (BioRad™) on a 1 mm thick (16 × 16 cm) polyacrylamide gel (acrylamide/bisacrylamide, 40%, 37,5:1, BioRad™) prepared with 1 × TAE buffer (pH 8, 40 mM de Tris Base, 20 mM acetic acid, 1 mM d'EDTA, MP Biomedicals™) and poured with a "Gradient maker" (Hoefer SG30®). For Saf-PARCH 519r*Cy3 PCR products, the 8% (w/v) polyacrylamide gel had a denaturant gradient between 30 and 60%. For $A344f^{GC}$-A915r*Cy3 PCR products, the 6% (w/v) polyacrylamide gel had a denaturant gradient between 40 and 70%. Electrophoresis was carried in 1 × TAE buffer at 60°C for 330 min at 200 V (initially at 80 V for 10 min). The gel was scanned using a Phospho fluorimager Typhoon 9400® (Amersham Biosciences™). Prior to band excision as described previously (Wilms et al., 2006), the gel was stained with SYBRGold® nucleic acid gel stain for 20 min, and washed for 10 min with 1 × TAE buffer and visualized with a Dark Reader transilluminator (Clare Chemicals, Dolores, CO). The DGGE profiles were analyzed by cluster analysis using the software package GelCompar II version 5.10 (Applied Maths, St-Martens-Latem, Belgium) as described elsewhere (Wilms et al., 2006).

Co-Migration-DGGE analysis (CM-DGGE)

Co-Migration-DGGE analysis (CM-DGGE), a new approach based on DGGE was developed in order to obtain the general archaeal depth diversity and associated active fraction. After amplification of the PCR products, using two different fluorescent reverse labelled primers from either total DNA or cDNA of the same sample, these were pooled and loaded into the same lane. Archaeal 16S rRNA gene amplification was performed with primers A344f^{GC}-A915r or Saf-PARCH 519r, labelled with either Cy3 or Cy5, following touchdown PCR protocol as previously described (Casamayor et al., 2000; Nicol et al., 2003). The DGGE analysis and gel conditions were the same as described for the DGGE analysis, except that loading and migration were performed in the dark. The gel was scanned using a Phospho fluorimager Typhoon 9400® (Amersham Biosciences™).

Cloning and sequencing

According to archaeal DGGE profiles, 21 DNA-derived 16SrRNA gene, two RNA-derived 16S rRNA gene and two DNA-derived *amoA* gene clone libraries were constructed. To minimize stochastic PCR bias (Polz and Cavanaugh, 1998), five independent PCR products were pooled, purified (QIAquick PCR purification Kit; Qiagen™), and cloned into *Escherichia coli* (XL10-Gold; Stratagene™) using the pGEM-T Easy vector system I (Promega™) following the manufacturer's instructions. Positive transformants were screened by PCR amplification of the insert using the vector-specific M13 primers. Plasmid extraction, purification and sequencing of the insert, were carried out by the sequencing Ouest-Genepole platform® of Roscoff Marine laboratory (France).

Phylogenetic analysis

Chimeras (Cole et al., 2003) were excluded from the clone libraries and a total of 771 sequences (including those from the 16S rRNA gene and *amoA* gene) were used for further phylogenetic analysis. The phylogenetic placement was carried out using NCBI BLAST search program within GenBank (http://www.ncbi.nlm.nih.gov/blast) (Altschul et al., 1990). The 16S rRNA sequences (~553 bases) were then edited in the BioEdit 7.0.5.3 program (Hall, 1999) and aligned using CLUSTALW (Thompson et al., 1994). The phylogenetic trees were constructed by the PHYLO_WIN program (Galtier et al., 1996) with neighbour-joining method (Saitou and Nei, 1987) and Jukes and Cantor correction. The *Thermococcales* dataset was further analyzed by Bayesian method. Bayesian trees were inferred using MrBayes 3.1.2. (Huelsenbeck and Ronquist, 2001). The Markov Chain Monte Carlo search was run with 4 chains for 2000000 generations, with trees being sampled every 100 generations. Stabilization of the chain parameters (tree likelihood, α shape parameter, and proportion of invariant sites) was verified with the program ModelTest version 3.7.2 (Posada and Crandall, 1998). The first 5000 trees were discarded (burn-in), keeping only trees generated after those parameters stabilized. Phylogenetic trees were viewed using the program TreeDyn (Chevenet et al., 2006). The nonchimeric *amoA* sequences (~635 bases) were translated into amino acids using BioEdit and then aligned using CLUSTALW, and the PHYLO_WIN program with neighbour-joining algorithm and PAM distance (Dayhoff et al., 1978) was then used for phylogenetic tree construction. For the 16S rRNA and *amoA* phylogenetic reconstruction, the robustness of inferred topology was tested by bootstrap resampling (1000), values over 50% are shown on the trees. The richness from the clone libraries was estimated, with the rarefaction curves at 99%, 97% and 95% sequence identity levels, using the DOTUR program (Schloss and Handelsman, 2005). Operational taxonomic units (OTUs), using a 97% sequence similarity, were generated with the SON program (Schloss and Handelsman, 2006), and the percentage of coverage (*Cx*) of the clone libraries was calculated by Good's method (Good, 1953) as described by Singleton and colleagues (Singleton et al., 2001). Statistical estimators, the significance of population differentiation among clone libraries (F_{ST}) (Martin, 2002), and the exact tests of population genetic differentiation (Raymond and Rousset, 1995), were calculated using Arlequin 3.11 (Excoffier et al., 2005).

Nucleotide sequence accession numbers

The sequences are available from GenBank database under the following accession numbers and names: 16S rRNA gene and rRNA (AM989356 to AM989452) and *amoA* gene (AM988840 to AM988859).

Acknowledgements

The authors are deeply indebted to Yvon Balut, chief of the operation on board the R.V. Marion Dufresne and to the I.P.E.V. (Institut Paul Emile Victor). We also thank Jean-Paul Foucher, chief scientist of ZoNéCo 12. All of the crew and the Scientific Party were crucial in this effort, especially Laetitia Hervé for the sampling efforts, and Frauke Klingelhoefer and Emmanuelle Cosquer for kindly providing the bathymetric map and seismic profiles. We are much indebted to anonymous referees for their helpful comments. This work was supported by the Université de Bretagne Occidentale, the Centre National de la Recherche Scientifique and the Région Bretagne. We are also grateful to Ouest-Génopole for the use of their facilities. Erwan Roussel was supported by a grant from the Ministère de la Recherche.

References

Altschul, S.F., Gish, W., Miller, W., Myers, E.W., and Lipman, D.J. (1990) Basic local alignment search tool. *J Mol Biol* **215**: 403-410.

Auzende, J.M., Van de Beuque, S., Dickens, G., Francois, C., Lavoy, Y., Voutay, O., and Exon, N. (2000) Deep sea diapirs and bottom simulating reflector in Fairway Basin (SW Pacific). *Marine Geophysical Researches* **21**: 579-587.

Biddle, J.F., Fitz-Gibbon, S., Schuster, S.C., Brenchley, J.E., and House, C.H. (2008) Metagenomic signatures of the Peru Margin subseafloor biosphere show a genetically distinct environment. *Proc Natl Acad Sci U S A* **105**: 10583-10588.

Biddle, J.F., Lipp, J.S., Lever, M.A., Lloyd, K.G., Sørensen, K.B., Anderson, R. et al. (2006) Heterotrophic *Archaea* dominate sedimentary subsurface ecosystems off Peru. *Proc Natl Acad Sci U S A* **103**: 3846-3851.

Bidle, K.A., Kastner, M., and Bartlett, D.H. (1999) A phylogenetic analysis of microbial communities associated with methane hydrate containing marine fluids and sediments in the Cascadia margin (ODP site 892B). *FEMS Microbiol Lett* **177**: 101-108.

Boetius, A., Ravenschlag, K., Schubert, C.J., Rickert, D., Widdel, F., Gieseke, A. et al. (2000) A marine microbial consortium apparently mediating anaerobic oxidation of methane. *Nature* **407**: 623-626.

Brochier-Armanet, C., Boussau, B., Gribaldo, S., and Forterre, P. (2008) Mesophilic *Crenarchaeota*: proposal for a third archaeal phylum, the *Thaumarchaeota*. *Nat Rev Microbiol* **6**: 245-252.

Casamayor, E.O., Schafer, H., Baneras, L., Pedros-Alio, C., and Muyzer, G. (2000) Identification of and spatio-temporal differences between microbial assemblages from two neighboring sulfurous lakes: comparison by microscopy and denaturing gradient gel electrophoresis. *Appl Environ Microbiol* **66**: 499-508.

Chevenet, F., Brun, C., Banuls, A.L., Jacq, B., and Christen, R. (2006) TreeDyn: towards dynamic graphics and annotations for analyses of trees. *BMC Bioinformatics* **7**: 439.

Cole, J.R., Chai, B., Marsh, T.L., Farris, R.J., Wang, Q., Kulam, S.A. et al. (2003) The Ribosomal Database Project (RDP-II): previewing a new autoaligner that allows regular updates and the new prokaryotic taxonomy. *Nucleic Acids Res* **31**: 442-443.

Cragg, B.A., Summit, M., and Parkes, R.J. (2000) Bacterial profiles in a sulfide mound (Site 1035) and an area of active fluid venting (Site 1036) in hot hydrothermal sediments from Middle Valley (Northeast Pacific). In *Proceedings of the Ocean Drilling Program, Scientific Results 169*. TX, United States: Texas A & M University, Ocean Drilling Program, College Station p. 18.

D'Hondt, S., Rutherford, S., and Spivack, A.J. (2002) Metabolic activity of subsurface life in deep-sea sediments. *Science* **295**: 2067-2070.

D'Hondt, S., Jorgensen, B.B., Miller, D.J., Batzke, A., Blake, R., Cragg, B.A. et al. (2004) Distributions of microbial activities in deep subseafloor sediments. *Science* **306**: 2216-2221.

Damste, J.S.S., and Coolen, M.J.L. (2006) Fossil DNA in cretaceous black shales: myth or reality? *Astrobiology* **6**: 299-302.

Danovaro, R., Dell'anno, A., Pusceddu, A., and Fabiano, M. (1999) Nucleic acid concentrations (DNA, RNA) in the continental and deep-sea sediments of the eastern Mediterranean: relationships with seasonally varying organic inputs and bacterial dynamics. *Deep-Sea Research Part I-Oceanographic Research Papers* **46**: 1077-1094.

Dayhoff, M.O., Schwartz, R.M., and Orcutt, B.C. (1978) A model of evolutionary change in proteins. In *Atlas of Protein Sequences and Structure*. Dayhoff, M.O. (ed). Washington DC: National Biomedical Research Foundation, pp. 345-352.

Dell'Anno, A., and Corinaldesi, C. (2004) Degradation and turnover of extracellular DNA in marine sediments: ecological and methodological considerations. *Appl Environ Microbiol* **70**: 4384-4386.

Dell'Anno, A., and Danovaro, R. (2005) Extracellular DNA plays a key role in deep-sea ecosystem functioning. *Science* **309**: 2179.

Dell'Anno, A., Fabiano, M., Duineveld, G.C.A., Kok, A., and Danovaro, R. (1998) Nucleic acid (DNA, RNA) quantification and RNA/DNA ratio determination in marine sediments: comparison of spectrophotometric, fluorometric, and HighPerformance liquid chromatography methods and estimation of detrital DNA. *Appl Environ Microbiol* **64**: 3238-3245.

Elshahed, M.S., Najar, F.Z., Roe, B.A., Oren, A., Dewers, T.A., and Krumholz, L.R. (2004) Survey of archaeal diversity reveals an abundance of halophilic *Archaea* in a low-salt, sulfide- and sulfur-rich spring. *Appl Environ Microbiol* **70**: 2230-2239.

Excoffier, L., Laval, G., and Schneider, S. (2005) Arlequin ver. 3.0: An integrated software package for population genetics data analysis. *Evol Bioinform Online* **1**: 47-50.

Foucher, J.P., Charlou, J.L., Harmegnies, F., Wirrmann, D., Sémah, A.M., Chaduteau, C., and Roussel, E. (2006) Rapport des travaux de la campagne ZoNéCo 12 : Campagne AUSFAIR/ZoNéCo12 à bord du N/O Marion Dufresne (12 au 26 février 2006). In: IFREMER.

Francis, C.A., Roberts, K.J., Beman, J.M., Santoro, A.E., and Oakley, B.B. (2005) Ubiquity and diversity of ammonia-oxidizing *Archaea* in water columns and sediments of the ocean. *Proc Natl Acad Sci U S A* **102**: 14683-14688.

Froelich, P.N., Klinkhammer, G.P., Bender, M.L., Luedtke, N.A., Heath, G.R., Cullen, D. et al. (1979) Early oxidation of organic-matter in pelagic sediments of the eastern equatorial atlantic-suboxic diagenesis. *Geochim Cosmochim Acta* **43**: 1075-1090.

Fry, J.C., Webster, G., Cragg, B.A., Weightman, A.J., and Parkes, R.J. (2006) Analysis of DGGE profiles to explore the relationship between prokaryotic community composition and biogeochemical processes in deep subseafloor sediments from the Peru Margin. *FEMS Microbiol Ecol* **58**: 86-98.

Fry, J.C., Parkes, R.J., Cragg, B.A., Weightman, A.J., and Webster, G. (2008) Prokaryotic biodiversity and activity in the deep subseafloor biosphere. *FEMS Microbiol Ecol* **66**: 181-196.

Galtier, N., Gouy, M., and Gautier, C. (1996) SEAVIEW and PHYLO_WIN: two graphic tools for sequence alignment and molecular phylogeny. *Comput Appl Biosci* **12**: 543-548.

Good, I.J. (1953) The population frequencies of species and the estimation of population parameters. *Biometrika* **40**: 237-264.

Hall, T.A. (1999) BioEdit: a user-friendly biological sequence alignment editor and analysis program for Windows 95/98/NT. *Nucleic Acids Symp Ser* **41**: 95-98.

Hallam, S.J., Mincer, T.J., Schleper, C., Preston, C.M., Roberts, K., Richardson, P.M., and DeLong, E.F. (2006) Pathways of carbon assimilation and ammonia oxidation suggested by environmental genomic analyses of marine *Crenarchaeota*. *PLoS Biol* **4**: 520-536.

Hinrichs, K.U., Hayes, J.M., Sylva, S.P., Brewer, P.G., and DeLong, E.F. (1999) Methane-consuming *Archaebacteria* in marine sediments. *Nature* **398**: 802-805.

Huelsenbeck, J.P., and Ronquist, F. (2001) MRBAYES: Bayesian inference of phylogenetic trees. *Bioinformatics* **17**: 754-755.

Inagaki, F., Takai, K., Komatsu, T., Kanamatsu, T., Fujioka, K., and Horikoshi, K. (2001) Archaeology of *Archaea*: geomicrobiological record of Pleistocene thermal events concealed in a deep-sea subseafloor environment. *Extremophiles* **5**: 385-392.

Inagaki, F., Suzuki, M., Takai, K., Oida, H., Sakamoto, T., Aoki, K. et al. (2003) Microbial communities associated with geological horizons in coastal subseafloor sediments from the sea of Okhotsk. *Appl Environ Microbiol* **69**: 7224-7235.

Inagaki, F., Nunoura, T., Nakagawa, S., Teske, A., Lever, M., Lauer, A. et al. (2006a) Biogeographical distribution and diversity of microbes in methane hydrate-bearing deep marine sediments on the Pacific Ocean Margin. *Proc Natl Acad Sci U S A* **103**: 2815-2820.

Inagaki, F., Kuypers, M.M., Tsunogai, U., Ishibashi, J., Nakamura, K., Treude, T. et al. (2006b) Microbial community in a sediment-hosted CO_2 lake of the southern Okinawa Trough hydrothermal system. *Proc Natl Acad Sci U S A* **103**: 14164-14169.

Jannasch, H.W., Wirsen, C.O., Molyneaux, S.J., and Langworthy, T.A. (1992) Comparative physiological-studies on hyperthermophilic *Archaea* isolated from deep-sea hot vents with emphasis on *Pyrococcus* strain Gb-D. *Appl Environ Microbiol* **58**: 3472-3481.

Kelley, D.S., Baross, J.A., and Delaney, J.R. (2002) Volcanoes, fluids, and life at mid-ocean ridge spreading centers. *Annu Rev Earth Planet Sci* **30**: 385-491.

Kemp, P.F., Lee, S., and Laroche, J. (1993) Estimating the growth rate of slowly growing marine bacteria from RNA content. *Appl Environ Microbiol* **59**: 2594-2601.

Kerkhof, L., and Ward, B.B. (1993) Comparison of nucleic acid hybridization and fluorometry for measurement of the relationship between RNA/DNA ratio and growth rate in a marine bacterium. *Appl Environ Microbiol* **59**: 1303-1309.

Könneke, M., Bernhard, A.E., de la Torre, J.R., Walker, C.B., Waterbury, J.B., and Stahl, D.A. (2005) Isolation of an autotrophic ammonia-oxidizing marine archaeon. *Nature* **437**: 543-546.

Kormas, K.A., Smith, D.C., Edgcomb, V., and Teske, A. (2003) Molecular analysis of deep subsurface microbial communities in Nankai Trough sediments (ODP Leg 190, Site 1176). *FEMS Microbiol Ecol* **45**: 115-125.

Kramer, J.G., and Singleton, F.L. (1993) Measurement of rRNA variations in natural communities of microorganisms on the southeastern U.S. continental shelf. *Appl Environ Microbiol* **59**: 2430-2436.

Lepage, E., Marguet, E., Geslin, C., Matte-Tailliez, O., Zillig, W., Forterre, P., and Tailliez, P. (2004) Molecular diversity of new Thermococcales isolates from a single area of hydrothermal deep-sea vents as revealed by randomly amplified polymorphic DNA fingerprinting and 16S rRNA gene sequence analysis. *Appl Environ Microbiol* **70**: 1277-1286.

Lipp, J.S., Morono, Y., Inagaki, F., and Hinrichs, K.-U. (2008) Significant contribution of *Archaea* to extant biomass in marine subsurface sediments. *Nature*. **454**: 991-994.

Lloyd, K.G., Lapham, L., and Teske, A. (2006) An anaerobic methane-oxidizing community of ANME-1b *Archaea* in hypersaline Gulf of Mexico sediments. *Appl Environ Microbiol* **72**: 7218-7230.

Martin, A.P. (2002) Phylogenetic approaches for describing and comparing the diversity of microbial communities. *Appl Environ Microbiol* **68**: 3673-3682.

Miroshnichenko, M.L., Hippe, H., Stackebrandt, E., Kostrikina, N.A., Chernyh, N.A., Jeanthon, C. et al. (2001) Isolation and characterization of *Thermococcus sibiricus* sp nov from a Western Siberia high-temperature oil reservoir. *Extremophiles* **5**: 85-91.

Muyzer, G. (1999) DGGE/TGGE a method for identifying genes from natural ecosystems. *Curr Opin Microbiol* **2**: 317-322.

Muyzer, G., and Stams, A.J.M. (2008) The ecology and biotechnology of sulphate-reducing bacteria. *Nat Rev Microbiol* **6**: 441-454.

Myers, R., Sheffield, V. and Cox, D. (1988) Detection of single base changes in DNA: ribonuclease cleavage and denaturing gradient gel electrophoresis. In *Genome Analysis. A Practical Approach*. Davies, K. (ed). Oxford: IRL Press, pp. 95-139.

Neufeld, J.D., and Mohn, W.W. (2005) Fluorophore-labeled primers improve the sensitivity, versatility, and normalization of denaturing gradient gel electrophoresis. *Appl Environ Microbiol* **71**: 4893-4896.

Newberry, C.J., Webster, G., Cragg, B.A., Parkes, J.R., Weighthman, A.J., and Fry, J.C. (2004) Diversity of prokaryotes and methanogenesis in deep subsurface sediments from Nankai Trough, ODP Leg 190. *Environ Microbiol* **6**: 274-287.

Nicol, G.W., Glover, L.A., and Prosser, J.I. (2003) The impact of grassland management on archaeal community structure in upland pasture rhizosphere soil. *Environ Microbiol* **5**: 152-162.

Parkes, R.J., Cragg, B.A., and Wellsbury, P. (2000) Recent studies on bacterial populations and processes in subfloor sediments: A review. *Hydrogeology Journal* **8**: 11-28.

Parkes, R.J., Webster, G., Cragg, B.A., Weightman, A.J., Newberry, C.J., Ferdelman, T.G. et al. (2005) Deep sub-seafloor prokaryotes stimulated at interfaces over geological time. *Nature* **436**: 390-394.

Pelletier, B., Chevillon, C., Menou, J.L., Butscher, J., Folcher, E., Geoffray, C. et al. (2006) Plongées, forage et cartographie Baie du Prony et Banc Gail, lagon Sud de Nouvelle-Calédonié, N.O.ALIS, 13-17 juin 2005 et cartographie Baie du Prony N.O.ALIS, 25-26 septembre 2005. In *Rapport de missions, Sci. Terre, Geol-Geophys*. Nouméa: Nouméa IRD, p. 44.

Polz, M.F., and Cavanaugh, C.M. (1998) Bias in template-to-product ratios in multitemplate PCR. *Appl Environ Microbiol* **64**: 3724-3730.

Posada, D., and Crandall, K.A. (1998) MODELTEST: testing the model of DNA substitution. *Bioinformatics* **14**: 817-818.

Preston, C.M., Wu, K.Y., Molinski, T.F., and DeLong, E.F. (1996) A psychrophilic crenarchaeon inhabits a marine sponge: *Cenarchaeum symbiosum* gen nov, sp, nov. *Proc Natl Acad Sci U S A* **93**: 6241-6246.

Purdy, K.J., Nedwell, D.B., and Embley, T.M. (2003) Analysis of the sulfate-reducing bacterial and methanogenic archaeal populations in contrasting Antarctic sediments. *Appl Environ Microbiol* **69**: 3181-3191.

Purdy, K.J., Munson, M.A., Nedwell, D.B., and Embley, T.M. (2002) Comparison of the molecular diversity of the methanogenic community at the brackish and marine ends of a UK estuary. *FEMS Microbiol Ecol* **39**: 17-21.

Raymond, M., and Rousset, F. (1995) An exact test for population differentiation. *Evolution* **49**: 1280-1283.

Roussel, E.G., Bonavita, M.-A.C., Querellou, J., Cragg, B.A., Webster, G., Prieur, D., and Parkes, R.J. (2008) Extending the sub-sea-floor biosphere. *Science* **320**: 1046.

Roussel, E.G., Sauvadet, A.-L., Allard, J., Chaduteau, C., Richard, P., Cambon Bonavita, M.-A., and Chaumillon, E. (2009) Archaeal methane cycling communities associated with gassy subsurface sediments of Marennes-Oléron Bay (France). *Geomicrobiol J* **26**: 31-43.

Saitou, N., and Nei, M. (1987) The neighbor-joining method: a new method for reconstructing phylogenetic trees. *Mol Biol Evol* **4**: 406-425.

Schippers, A., Neretin, L.N., Kallmeyer, J., Ferdelman, T.G., Cragg, B.A., John Parkes, R., and Jorgensen, B.B. (2005) Prokaryotic cells of the deep sub-seafloor biosphere identified as living bacteria. *Nature* **433**: 861-864.

Schloss, P.D., and Handelsman, J. (2004) Status of the microbial census. *Microbiol Mol Biol Rev* **68**: 686-691.

Schloss, P.D., and Handelsman, J. (2005) Introducing DOTUR, a computer program for defining operational taxonomic units and estimating species richness. *Appl Environ Microbiol* **71**: 1501-1506.

Schloss, P.D., and Handelsman, J. (2006) Introducing SONS, a tool for operational taxonomic unit-based comparisons of microbial community memberships and structures. *Appl Environ Microbiol* **72**: 6773-6779.

Sheffield, V.C., Cox, D.R., Lerman, L.S., and Myers, R.M. (1989) Attachment of a 40-base-pair G + C-rich sequence (GC-clamp) to genomic DNA fragments by the polymerase chain reaction results in improved detection of single-base changes. *Proc Natl Acad Sci U S A* **86**: 232-236.

Singh, N., Kendall, M.M., Liu, Y.T., and Boone, D.R. (2005) Isolation and characterization of methylotrophic methanogens from anoxic marine sediments in Skan Bay, Alaska: description of *Methanococcoides alaskense* sp nov., and emended description of *Methanosarcina baltica*. *Int J Syst Evol Microbiol* **55**: 2531-2538.

Singleton, D.R., Furlong, M.A., Rathbun, S.L., and Whitman, W.B. (2001) Quantitative comparisons of 16S rRNA gene sequence libraries from environmental samples. *Appl Environ Microbiol* **67**: 4374-4376.

Sivan, O., Schrag, D.P., and Murray, R.W. (2007) Rates of methanogenesis and methanotrophy in deep-sea sediments. *Geobiology* **5**: 141-151.

Smalla, K., Oros-Sichler, M., Milling, A., Heuer, H., Baumgarte, S., Becker, R. et al. (2007) Bacterial diversity of soils assessed by DGGE, T-RFLP and SSCP fingerprints of PCR-amplified 16S rRNA gene fragments: Do the different methods provide similar results? *J Microbiol Methods* **69**: 470-479.

Sørensen, K.B., and Teske, A. (2006) Stratified communities of active *Archaea* in deep marine subsurface sediments. *Appl Environ Microbiol* **72**: 4596-4603.

Sørensen, K.B., Lauer, A., and Teske, A. (2004) Archaeal phylotypes in a metal-rich and low-activity deep subsurface sediment of the Peru Basin, ODP Leg 201, Site 1231. *Geobiology* **2**: 151-161.

Stahl, D.A., and Amann, R.I. (1991) Development and application of nucleic acid probes in bacterial systematics. In Nucleic Acid Techniques in Bacterial Systematics. Stackebrandt, E., and Goodfellow, M. (eds). Chichester: John Wiley and Sons, pp. 205-248.

Summit, M., and Baross, J.A. (2001) A novel microbial habitat in the mid-ocean ridge subseafloor. *Proc Natl Acad Sci U S A* **98**: 2158-2163.

Suzuki, M.T., and Giovannoni, S.J. (1996) Bias caused by template annealing in the amplification of mixtures of 16S rRNA genes by PCR. *Appl Environ Microbiol* **62**: 625-630.

Takai, K., and Horikoshi, K. (1999) Genetic diversity of *Archaea* in deep-sea hydrothermal vent environments. *Genetics* **152**: 1285-1297.

Teske, A., and Sørensen, K.B. (2008) Uncultured *Archaea* in deep marine subsurface sediments: have we caught them all? *ISME J* **2**: 3-18.

Teske, A., Hinrichs, K.U., Edgcomb, V., de Vera Gomez, A., Kysela, D., Sylva, S.P. et al. (2002) Microbial diversity of hydrothermal sediments in the Guaymas Basin: evidence for anaerobic methanotrophic communities. *Appl Environ Microbiol* **68**: 1994-2007.

Thiel, M., and Gutow, L. (2005) The ecology of rafting in the marine environment - I - The floating substrata. In *Oceanography and Marine Biology: An Annual Review, Vol 42*, pp. 181-263.

Thiel, M., and Haye, P.A. (2006) The ecology of rafting in the marine environment. III. Biogeographical and evolutionary consequences. In *Oceanography and Marine Biology - an Annual Review, Vol 44*, pp. 323-429.

Thompson, J.D., Higgins, D.G., and Gibson, T.J. (1994) CLUSTAL W: improving the sensitivity of progressive multiple sequence alignment through sequence weighting, position-specific gap penalties and weight matrix choice. *Nucleic Acids Res* **22**: 4673-4680.

Treude, T., Kruger, M., Boetius, A., and Jorgensen, B.B. (2005) Environmental control on anaerobic oxidation of methane in the gassy sediments of Eckernforde Bay (German Baltic). *Limnol Oceanogr* **50**: 1771-1786.

Valentine, D.L. (2007) Adaptations to energy stress dictate the ecology and evolution of the *Archaea*. *Nat Rev Microbiol* **5**: 316-323.

von Wintzingerode, F., Gobel, U.B., and Stackebrandt, E. (1997) Determination of microbial diversity in environmental samples: pitfalls of PCR-based rRNA analysis. *FEMS Microbiol Rev* **21**: 213-229.

Webster, G., Newberry, C.J., Fry, J.C., and Weightman, A.J. (2003) Assessment of bacterial community structure in the deep sub-seafloor biosphere by 16S rDNA-based techniques: a cautionary tale. *J Microbiol Methods* **55**: 155-164.

Webster, G., Blazejak, A., Cragg, B.A., Schippers, A., Sass, H., Rinna, J. et al. (2008) Subsurface microbiology and biogeochemistry of a deep, cold-water carbonate mound from the Porcupine Seabight (IODP Expedition 307). *Environ Microbiol* **11**: 239-257.

Wellsbury, P., Mather, I., and Parkes, R.J. (2002) Geomicrobiology of deep, low organic carbon sediments in the Woodlark Basin, Pacific Ocean. *FEMS Microbiol Ecol* **42**: 59-70.

Whitman, W.B., Coleman, D.C., and Wiebe, W.J. (1998) Prokaryotes: The unseen majority. *Proc Natl Acad Sci U S A* **95**: 6578-6583.

Wilms, R., Kopke, B., Sass, H., Chang, T.S., Cypionka, H., and Engelen, B. (2006) Deep biosphere-related bacteria within the subsurface of tidal flat sediments. *Environ Microbiol* **8**: 709-719.

Captions

Fig. 1. Bathymetric map of the location of ZoNéCo 12 sites. The white arrow represents substantial amounts of terrigenous matter derived from New Caledonia.

Fig. 2. Geochemical and total prokaryote cell depth profiles of the sediments from the Fairway and New Caledonia Basin sites.

Fig. 3. Depth distribution of the archaeal phylogenetic community structures based on 16S rRNA gene from the Fairway and New Caledonia Basin sites. According to archaeal DGGE profiles (DGGE), clone libraries were only constructed for the depths with the most representative archaeal phylogenetic distribution for each core. The phylogenetic affiliation of each clone sequence was determined by similarity analysis. The relative abundance of each phylotype was calculated and represented in a column diagram. The percentage of coverage of each clone library examined is indicated in brackets. The asterisks indicate groups of clone libraries with insignificant ($P < 0.01$) differences between all the diversity indices (F_{ST} and the exact test method). ANME-2: *an*aerobic *me*thane oxidizers group 2, NMG-1: Novel *Methanosarcinales* group 1, SAGMEG: South African Gold Mine Euryarchaeotic Group, DHVE6: Deep-Sea Hydrothermal Vent Euryarchaeotal Group 6.

Fig. 4. Phylogenetic tree representing the Marine Group 1 (MG-1) 16S rRNA gene sequences DNA- and RNA-derived. Each phylotype from each clone library is represented by one sequence with ≥97% similarity grouping. The tree was constructed using the neighbour-joining method with Jukes and Cantor correction. Bootstrap values <50% are not shown. Sequences are color-coded according to site location. Sequences from RNA-derived clone libraries were underlined.

Fig. 5. Co-migration denaturant gradient gel electrophoresis (CM-DGGE) analysis of archaeal 16S rRNA genes DNA-derived (blue) and RNA-derived (red) from MD06-3018 and MD06-3019 sites. The numbered bands were excised and sequenced. The lineage and the sequence similarity of the closest match by BLASTN search are given on the right. PCR products were amplified with the Saf-PARCH 519r*Cy5 (blue) or Saf-PARCH 519r*Cy3 (red) primer set and electrophoresis was performed using a gradient of 30–60% denaturant.

Fig. 6. Phylogenetic tree based on translated, partial amino acid sequences of *amoA* gene (<212 amino acids). The tree was constructed using the neighbour-joining method using PAM distance (Dayhoff et al., 1978). The robustness of inferred topology was tested by the bootstrap. Bootstrap values <50% are not shown. Sequences are color-coded according to location (blue, sediment; red, seawater; brown, soil) and were clustered as previously published (Francis et al., 2005). Sequences retrieved from the New Caledonia Basin are in black.

Fig. 7. Phylogenetic tree representing the *Thermococcus* 16S rRNA gene sequences from the Fairway and New Caledonia Basin sites. Tree topology was inferred by neighbour-joining analysis on ~550 bases with Jukes and Cantor correction. Bootstrap support values over 50% (1,000 replicates) and bayesian posterior probabilities are indicated at nodes. Closely related sequence clusters are represented by single sequences. TG-1: *Thermococcales Group 1*, DSSTG: *Deep Sub-Seafloor Thermococcales Group*. Sequences are color-coded according to the clone library.

Supplementary material

Fig. S1. Seismic profiles of the Fairway Basin with the location of each site: MD06-3022, MD06-3026, MD06-3027 and MD06-3028. Figure modified from Foucher et al. (2006).

Fig. S2. Denaturant gradient gel electrophoresis (DGGE) analysis of archaeal 16S rRNA genes of the cores from the Fairway and New Caledonia Basin sites. The numbered bands were excised and sequenced. The lineage and the sequence similarity of the closest match by BLASTN search are given on the right. (A) PCR products were amplified with the A344f^{GC}-A915r primer set and electrophoresis was performed using a gradient of 40–70% denaturant. (B) PCR products were amplified with the Saf-PARCH 519r primer set and electrophoresis was performed using a gradient of 30–60% denaturant. (C) Cluster analysis of DGGE band patterns. The dendrogram was calculated by Pearson correlation and UPGMA.

Fig. S3. Rarefaction curves for the 16S rRNA gene clone libraries from the Fairway and New Caledonia Basin sites (Schloss and Handelsman, 2005). The sequence identity levels are represented in brackets.

Fig. S4. Phylogenetic tree representing the *Euryarchaeota* 16S rRNA gene, except the *Thermococcales* lineage, sequences DNA- and RNA derived. RNA-derived sequences are underlined. Each phylotype is represented by one sequence with ≥97% similarity grouping. The tree was constructed using the neighbour-joining method with Jukes and Cantor correction. Bootstrap values <50% are not shown. ANME: *an*aerobic *me*thane oxidizers, NMG-1: Novel *Methanosarcinales* group 1, SAGMEG: South African Gold Mine Euryarchaeotic Group, DHVE6: Deep-Sea Hydrothermal Vent Euryarchaeotal Group 6, MBG-D: Marine Benthic Group D, MG: Marine Groups. Sequences are color-coded according to site location.

Fig. S5. Phylogenetic tree representing the *Crenarchaeota* 16S rRNA gene sequences, except the MG-1 lineage, DNA- and RNA derived. RNA-derived sequences are underlined. Each phylotype is represented by one sequence with ≥97% similarity grouping. The tree was constructed using the neighbour-joining method with Jukes and Cantor correction. Bootstrap values <50% are not shown. MCG: Miscellaneous Crenarchaeotal Group, MBG-B: Marine Benthic Group B, MBG-A: Marine Benthic Group A. Sequences are color-coded according to site location.

Fig. S6. *C*o-*M*igration *D*enaturant *G*radient *G*el *E*lectrophoresis (CM-DGGE) analysis of archaeal 16S rRNA genes DNA-derived (blue) and RNA-derived (red) from the cores at MD06-3018 and MD06-3019 sites. The numbered bands were excised and sequenced. The lineage and the sequence similarity of the closest match by BLASTN search are given on the right. PCR products were amplified with the A344f^{GC}-A915r*Cy5 (blue) or A344f^{GC}-A915r*Cy3 (red) primer set and electrophoresis was performed using a gradient of 40–70% denaturant. (A) DNA-derived (A344f^{GC}-A915r*Cy5). (B) RNA-derived (A344f^{GC}-A915r*Cy3). (C) both DNA- and RNA-derived.

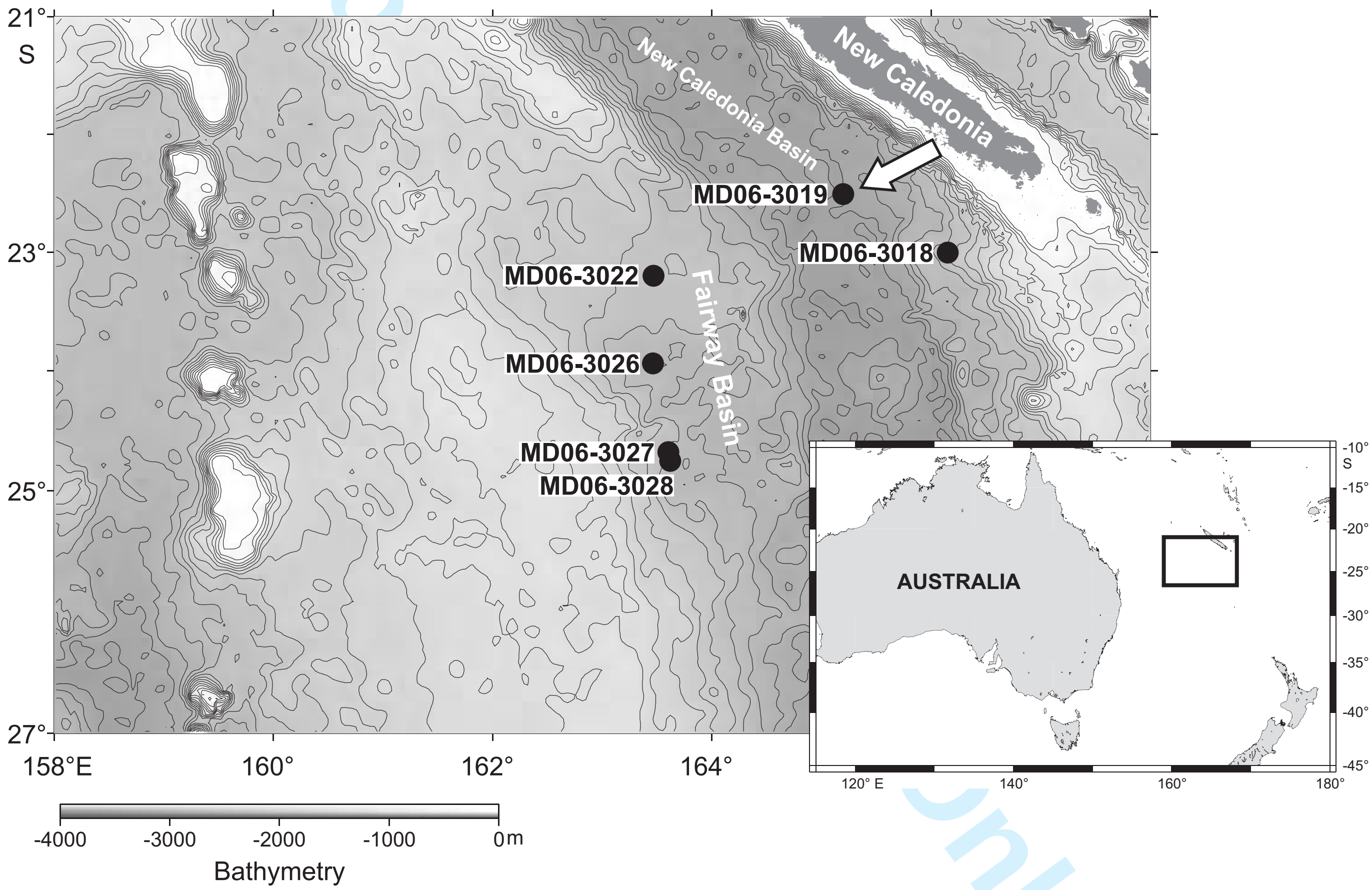
New Caledonia
New Caledonia Basin
Fairway Basin
MD06-3019
MD06-3018
MD06-3022
MD06-3026
MD06-3027
MD06-3028
21° S
23°
25°
27°
158°E
160°
162°
164°
AUSTRALIA
120° E
140°
160°
180°
-10° S
-15°
-20°
-25°
-30°
-35°
-40°
-45°
-4000
-3000
-2000
-1000
0 m
Bathymetry

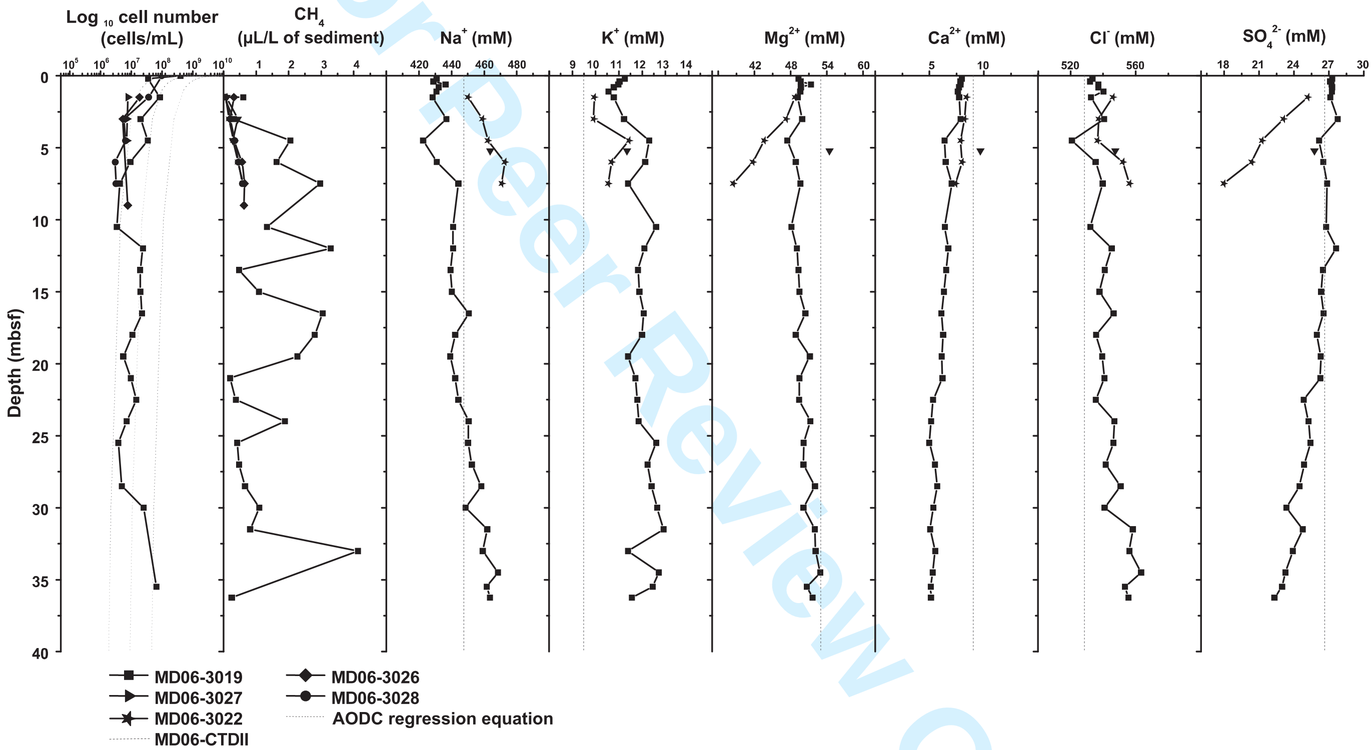

Log 10 cell number (cells/mL)
CH4 (μL/L of sediment)
Na+ (mM)
K+ (mM)
Mg2+ (mM)
Ca2+ (mM)
Cl- (mM)
SO42- (mM)
Depth (mbsf)
MD06-3019
MD06-3027
MD06-3022
MD06-CTDII
MD06-3026
MD06-3028
AODC regression equation

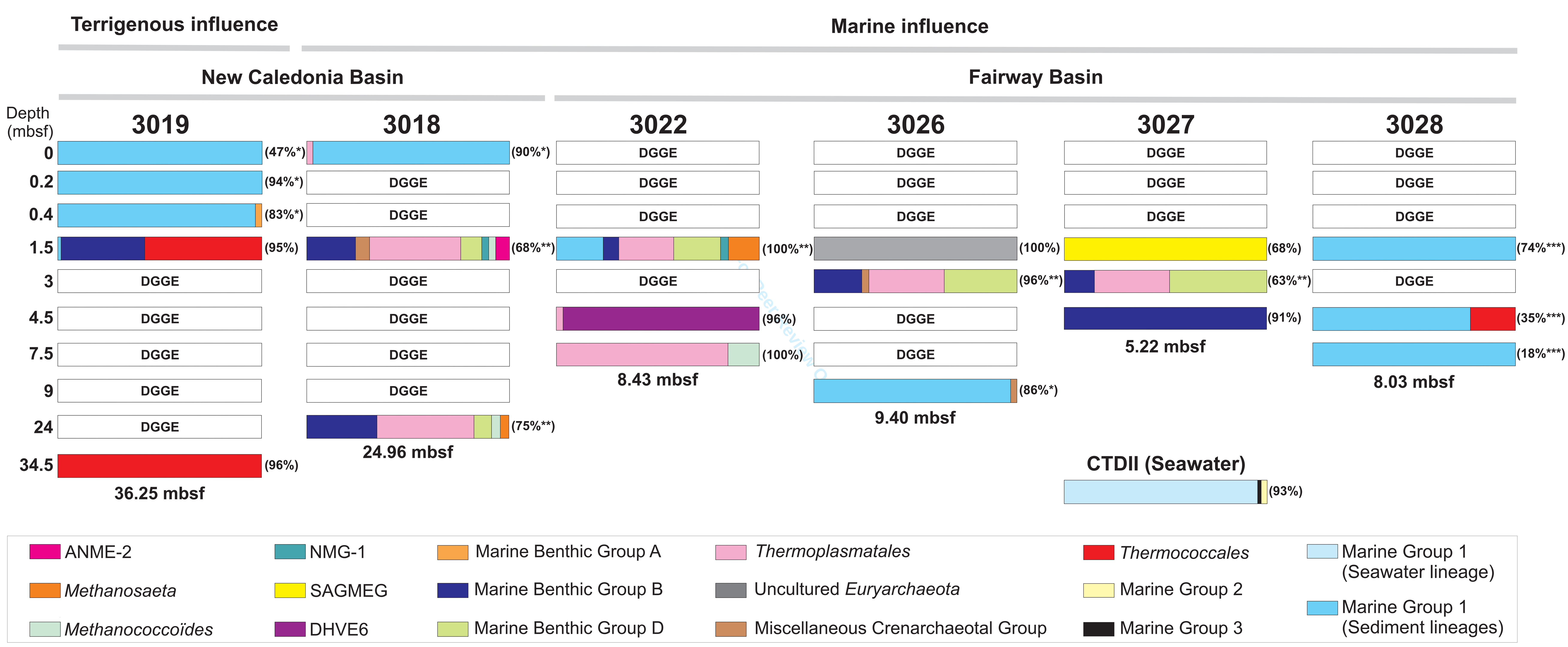
Terrigenous influence
Marine influence
New Caledonia Basin
Fairway Basin
Depth (mbsf)
3019
3018
3022
3026
3027
3028
0
0.2
0.4
1.5
3
4.5
7.5
9
24
34.5
DGGE
(47%*)
(94%*)
(83%*)
(95%)
(96%)
36.25 mbsf
(90%*)
(68%**)
(75%**)
24.96 mbsf
(100%**)
(96%)
(100%)
8.43 mbsf
(100%)
(96%**)
(86%*)
9.40 mbsf
(68%)
(63%**)
(91%)
5.22 mbsf
(74%***)
(35%***)
(18%***)
8.03 mbsf
CTDII (Seawater)
(93%)
ANME-2
Methanosaeta
Methanococcoïdes
NMG-1
SAGMEG
DHVE6
Marine Benthic Group A
Marine Benthic Group B
Marine Benthic Group D
Thermoplasmatales
Uncultured Euryarchaeota
Miscellaneous Crenarchaeotal Group
Thermococcales
Marine Group 2
Marine Group 3
Marine Group 1 (Seawater lineage)
Marine Group 1 (Sediment lineages)

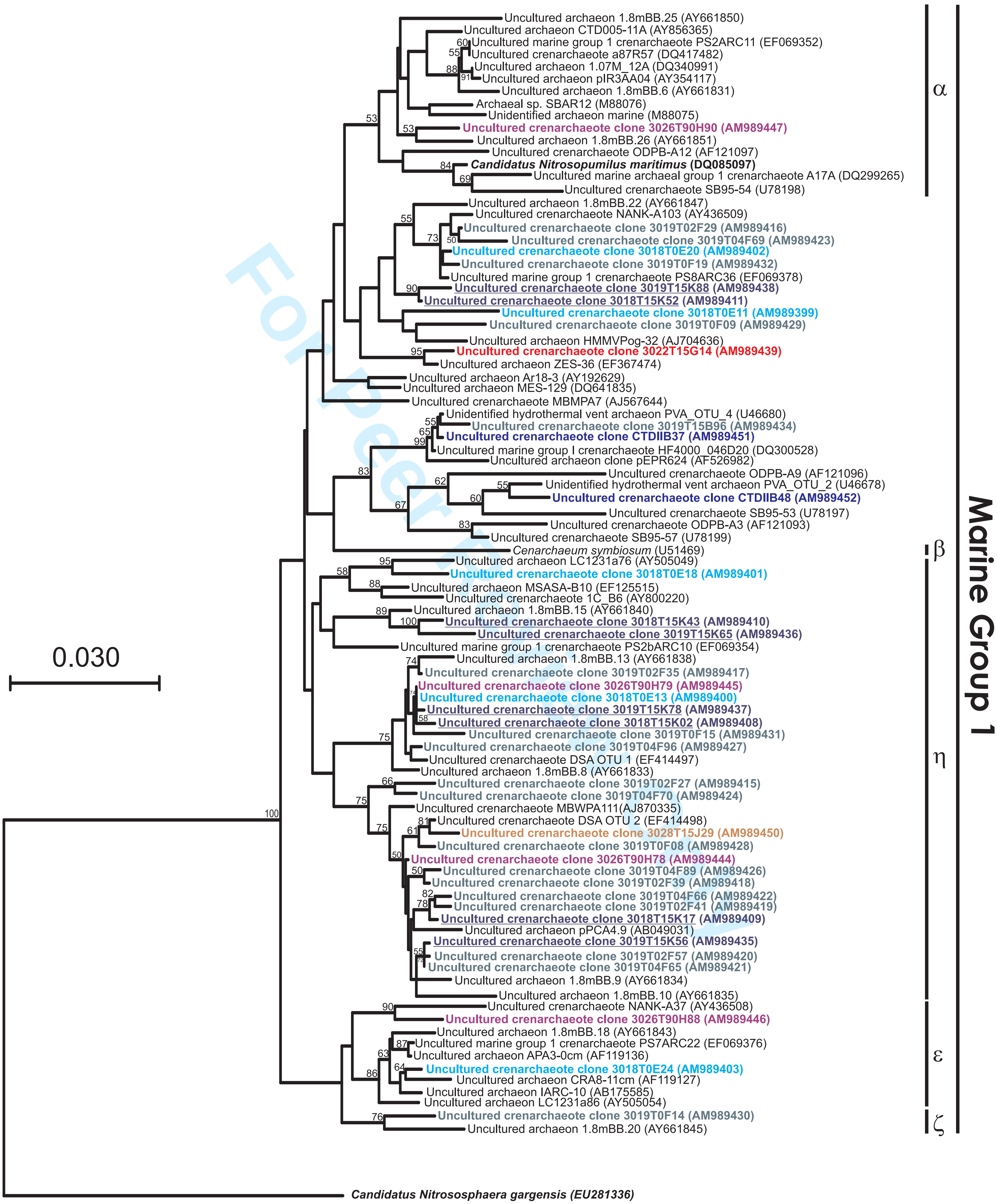
Uncultured archaeon 1.8mBB.25 (AY661850)
Uncultured archaeon CTD005-11A (AY856365)
Uncultured marine group 1 crenarchaeote PS2ARC11 (EF069352)
Uncultured crenarchaeote a87R57 (DQ417482)
Uncultured archaeon 1.07M_12A (DQ340991)
Uncultured archaeon pIR3AA04 (AY354117)
Uncultured archaeon 1.8mBB.6 (AY661831)
Archaeal sp. SBAR12 (M88076)
Unidentified archaeon marine (M88075)
Uncultured crenarchaeote clone 3026T90H90 (AM989447)
Uncultured archaeon 1.8mBB.26 (AY661851)
Uncultured crenarchaeote ODPB-A12 (AF121097)
Candidatus Nitrosopumilus maritimus (DQ085097)
Uncultured marine archaeal group 1 crenarchaeote A17A (DQ299265)
Uncultured crenarchaeote SB95-54 (U78198)
Uncultured archaeon 1.8mBB.22 (AY661847)
Uncultured crenarchaeote NANK-A103 (AY436509)
Uncultured crenarchaeote clone 3019T02F29 (AM989416)
Uncultured crenarchaeote clone 3019T04F69 (AM989423)
Uncultured crenarchaeote clone 3018T0E20 (AM989402)
Uncultured crenarchaeote clone 3019T0F19 (AM989432)
Uncultured marine group 1 crenarchaeote PS8ARC36 (EF069378)
Uncultured crenarchaeote clone 3019T15K88 (AM989438)
Uncultured crenarchaeote clone 3018T15K52 (AM989411)
Uncultured crenarchaeote clone 3018T0E11 (AM989399)
Uncultured crenarchaeote clone 3019T0F09 (AM989429)
Uncultured archaeon HMMVPog-32 (AJ704636)
Uncultured crenarchaeote clone 3022T15G14 (AM989439)
Uncultured archaeon ZES-36 (EF367474)
Uncultured archaeon Ar18-3 (AY192629)
Uncultured archaeon MES-129 (DQ641835)
Uncultured crenarchaeote MBMPA7 (AJ567644)
Unidentified hydrothermal vent archaeon PVA_OTU_4 (U46680)
Uncultured crenarchaeote clone 3019T15B96 (AM989434)
Uncultured crenarchaeote clone CTDIIB37 (AM989451)
Uncultured marine group I crenarchaeote HF4000_046D20 (DQ300528)
Uncultured archaeon clone pEPR624 (AF526982)
Uncultured crenarchaeote ODPB-A9 (AF121096)
Unidentified hydrothermal vent archaeon PVA_OTU_2 (U46678)
Uncultured crenarchaeote clone CTDIIB48 (AM989452)
Uncultured crenarchaeote SB95-53 (U78197)
Uncultured crenarchaeote ODPB-A3 (AF121093)
Uncultured crenarchaeote SB95-57 (U78199)
Cenarchaeum symbiosum (U51469)
Uncultured archaeon LC1231a76 (AY505049)
Uncultured crenarchaeote clone 3018T0E18 (AM989401)
Uncultured archaeon MSASA-B10 (EF125515)
Uncultured crenarchaeote 1C_B6 (AY800220)
Uncultured archaeon 1.8mBB.15 (AY661840)
Uncultured crenarchaeote clone 3018T15K43 (AM989410)
Uncultured crenarchaeote clone 3019T15K65 (AM989436)
Uncultured marine group 1 crenarchaeote PS2bARC10 (EF069354)
Uncultured archaeon 1.8mBB.13 (AY661838)
Uncultured crenarchaeote clone 3019T02F35 (AM989417)
Uncultured crenarchaeote clone 3026T90H79 (AM989445)
Uncultured crenarchaeote clone 3018T0E13 (AM989400)
Uncultured crenarchaeote clone 3019T15K78 (AM989437)
Uncultured crenarchaeote clone 3018T15K02 (AM989408)
Uncultured crenarchaeote clone 3019T0F15 (AM989431)
Uncultured crenarchaeote clone 3019T04F96 (AM989427)
Uncultured crenarchaeote DSA OTU 1 (EF414497)
Uncultured archaeon 1.8mBB.8 (AY661833)
Uncultured crenarchaeote clone 3019T02F27 (AM989415)
Uncultured crenarchaeote clone 3019T04F70 (AM989424)
Uncultured crenarchaeote MBWPA111(AJ870335)
Uncultured crenarchaeote DSA OTU 2 (EF414498)
Uncultured crenarchaeote clone 3028T15J29 (AM989450)
Uncultured crenarchaeote clone 3019T0F08 (AM989428)
Uncultured crenarchaeote clone 3026T90H78 (AM989444)
Uncultured crenarchaeote clone 3019T04F89 (AM989426)
Uncultured crenarchaeote clone 3019T02F39 (AM989418)
Uncultured crenarchaeote clone 3019T04F66 (AM989422)
Uncultured crenarchaeote clone 3019T02F41 (AM989419)
Uncultured crenarchaeote clone 3018T15K17 (AM989409)
Uncultured archaeon pPCA4.9 (AB049031)
Uncultured crenarchaeote clone 3019T15K56 (AM989435)
Uncultured crenarchaeote clone 3019T02F57 (AM989420)
Uncultured crenarchaeote clone 3019T04F65 (AM989421)
Uncultured archaeon 1.8mBB.9 (AY661834)
Uncultured archaeon 1.8mBB.10 (AY661835)
Uncultured crenarchaeote NANK-A37 (AY436508)
Uncultured crenarchaeote clone 3026T90H88 (AM989446)
Uncultured archaeon 1.8mBB.18 (AY661843)
Uncultured marine group 1 crenarchaeote PS7ARC22 (EF069376)
Uncultured archaeon APA3-0cm (AF119136)
Uncultured crenarchaeote clone 3018T0E24 (AM989403)
Uncultured archaeon CRA8-11cm (AF119127)
Uncultured archaeon IARC-10 (AB175585)
Uncultured archaeon LC1231a86 (AY505054)
Uncultured crenarchaeote clone 3019T0F14 (AM989430)
Uncultured archaeon 1.8mBB.20 (AY661845)
Candidatus Nitrososphaera gargensis (EU281336)
0.030
α
β
η
ε
ζ
Marine Group 1

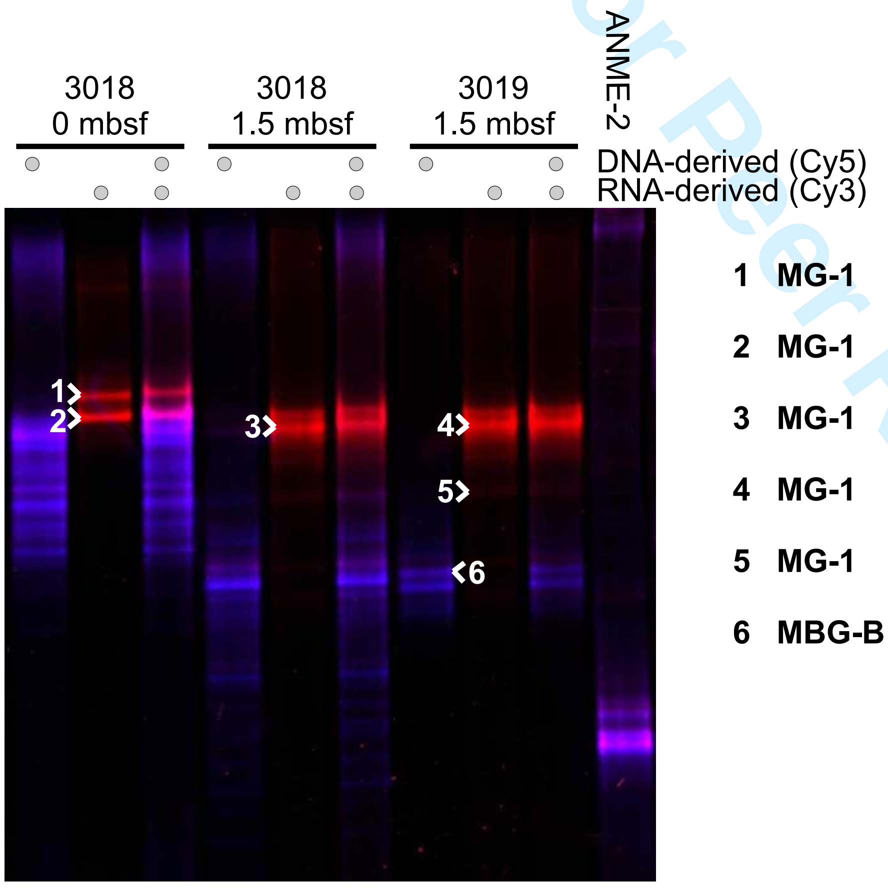

1 **MG-1** (Unc. *crenarchaeote* clone aEPR13S145 - EU259329 - 90%)

2 **MG-1** (Unc. *crenarchaeote* clone aEPR13S145 - EU259329 - 96%)

3 **MG-1** (Unc. *crenarchaeote* clone 1.8mBB.9 - AY661834 - 92%)

4 **MG-1** (Unc. *crenarchaeote* clone MD2902-A18 - EU048603 - 89%)

5 **MG-1** (Unc. *crenarchaeote* clone arc3. - AJ783668 - 89%)

6 **MBG-B** (Unc. *crenarchaeote* clone MD2896-0.1m.4 - DQ984881 - 100%)

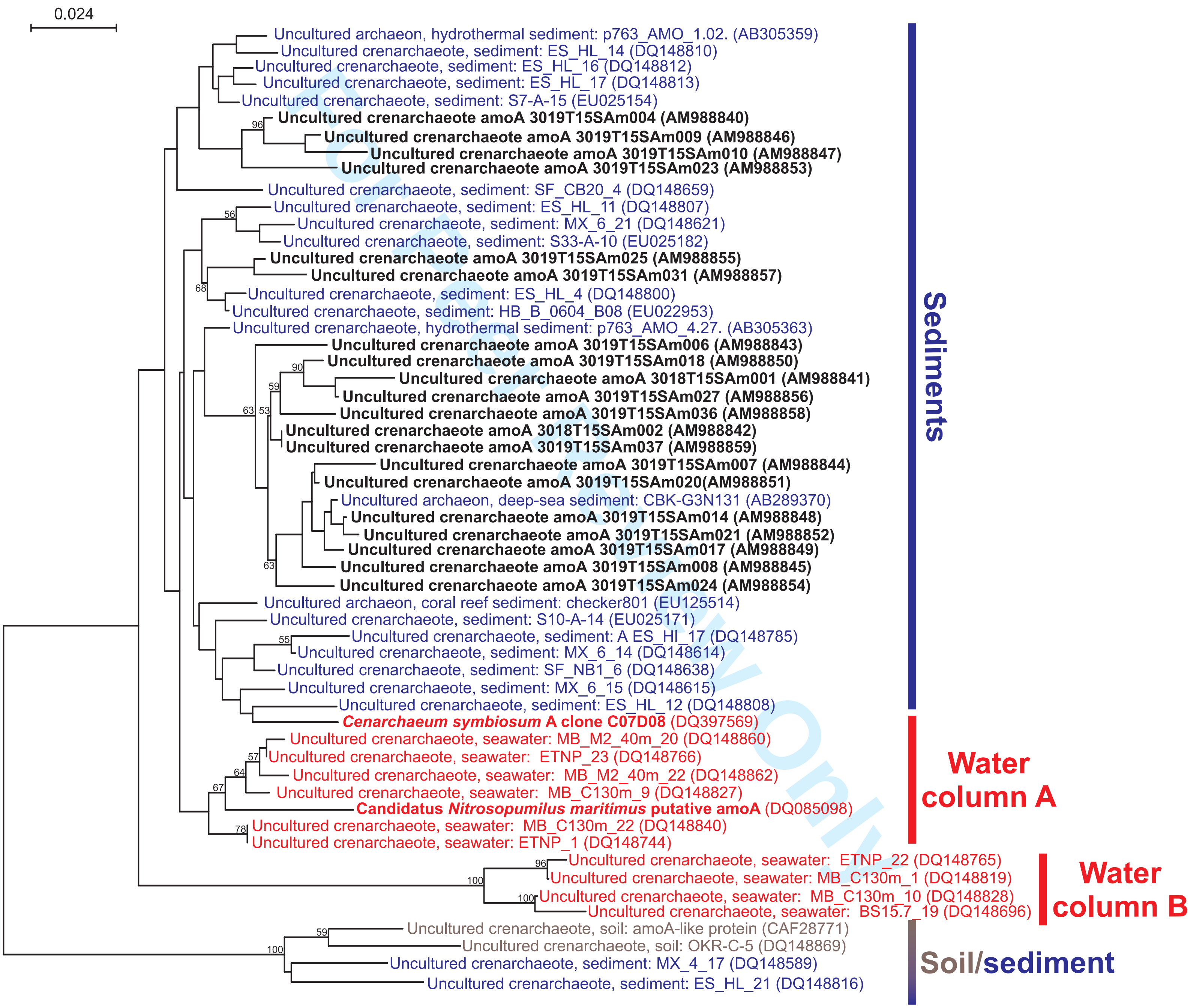
0.024
Uncultured archaeon, hydrothermal sediment: p763_AMO_1.02. (AB305359)
Uncultured crenarchaeote, sediment: ES_HL_14 (DQ148810)
Uncultured crenarchaeote, sediment: ES_HL_16 (DQ148812)
Uncultured crenarchaeote, sediment: ES_HL_17 (DQ148813)
Uncultured crenarchaeote, sediment: S7-A-15 (EU025154)
96
Uncultured crenarchaeote amoA 3019T15SAm004 (AM988840)
Uncultured crenarchaeote amoA 3019T15SAm009 (AM988846)
Uncultured crenarchaeote amoA 3019T15SAm010 (AM988847)
Uncultured crenarchaeote amoA 3019T15SAm023 (AM988853)
Uncultured crenarchaeote, sediment: SF_CB20_4 (DQ148659)
56
Uncultured crenarchaeote, sediment: ES_HL_11 (DQ148807)
Uncultured crenarchaeote, sediment: MX_6_21 (DQ148621)
Uncultured crenarchaeote, sediment: S33-A-10 (EU025182)
Uncultured crenarchaeote amoA 3019T15SAm025 (AM988855)
Uncultured crenarchaeote amoA 3019T15SAm031 (AM988857)
68
Uncultured crenarchaeote, sediment: ES_HL_4 (DQ148800)
Uncultured crenarchaeote, sediment: HB_B_0604_B08 (EU022953)
Uncultured crenarchaeote, hydrothermal sediment: p763_AMO_4.27. (AB305363)
Uncultured crenarchaeote amoA 3019T15SAm006 (AM988843)
90
Uncultured crenarchaeote amoA 3019T15SAm018 (AM988850)
59
Uncultured crenarchaeote amoA 3018T15SAm001 (AM988841)
Uncultured crenarchaeote amoA 3019T15SAm027 (AM988856)
63 53
Uncultured crenarchaeote amoA 3019T15SAm036 (AM988858)
Uncultured crenarchaeote amoA 3018T15SAm002 (AM988842)
Uncultured crenarchaeote amoA 3019T15SAm037 (AM988859)
Uncultured crenarchaeote amoA 3019T15SAm007 (AM988844)
Uncultured crenarchaeote amoA 3019T15SAm020(AM988851)
Uncultured archaeon, deep-sea sediment: CBK-G3N131 (AB289370)
Uncultured crenarchaeote amoA 3019T15SAm014 (AM988848)
Uncultured crenarchaeote amoA 3019T15SAm021 (AM988852)
Uncultured crenarchaeote amoA 3019T15SAm017 (AM988849)
63
Uncultured crenarchaeote amoA 3019T15SAm008 (AM988845)
Uncultured crenarchaeote amoA 3019T15SAm024 (AM988854)
Uncultured archaeon, coral reef sediment: checker801 (EU125514)
Uncultured crenarchaeote, sediment: S10-A-14 (EU025171)
55
Uncultured crenarchaeote, sediment: A ES_HI_17 (DQ148785)
Uncultured crenarchaeote, sediment: MX_6_14 (DQ148614)
Uncultured crenarchaeote, sediment: SF_NB1_6 (DQ148638)
Uncultured crenarchaeote, sediment: MX_6_15 (DQ148615)
Uncultured crenarchaeote, sediment: ES_HL_12 (DQ148808)
Cenarchaeum symbiosum A clone C07D08 (DQ397569)
Uncultured crenarchaeote, seawater: MB_M2_40m_20 (DQ148860)
57
Uncultured crenarchaeote, seawater: ETNP_23 (DQ148766)
64
Uncultured crenarchaeote, seawater: MB_M2_40m_22 (DQ148862)
67
Uncultured crenarchaeote, seawater: MB_C130m_9 (DQ148827)
Candidatus Nitrosopumilus maritimus putative amoA (DQ085098)
78
Uncultured crenarchaeote, seawater: MB_C130m_22 (DQ148840)
Uncultured crenarchaeote, seawater: ETNP_1 (DQ148744)
96
Uncultured crenarchaeote, seawater: ETNP_22 (DQ148765)
Uncultured crenarchaeote, seawater: MB_C130m_1 (DQ148819)
100
100
Uncultured crenarchaeote, seawater: MB_C130m_10 (DQ148828)
Uncultured crenarchaeote, seawater: BS15.7_19 (DQ148696)
59
Uncultured crenarchaeote, soil: amoA-like protein (CAF28771)
100
Uncultured crenarchaeote, soil: OKR-C-5 (DQ148869)
Uncultured crenarchaeote, sediment: MX_4_17 (DQ148589)
Uncultured crenarchaeote, sediment: ES_HL_21 (DQ148816)
Sediments
Water column A
Water column B
Soil/sediment

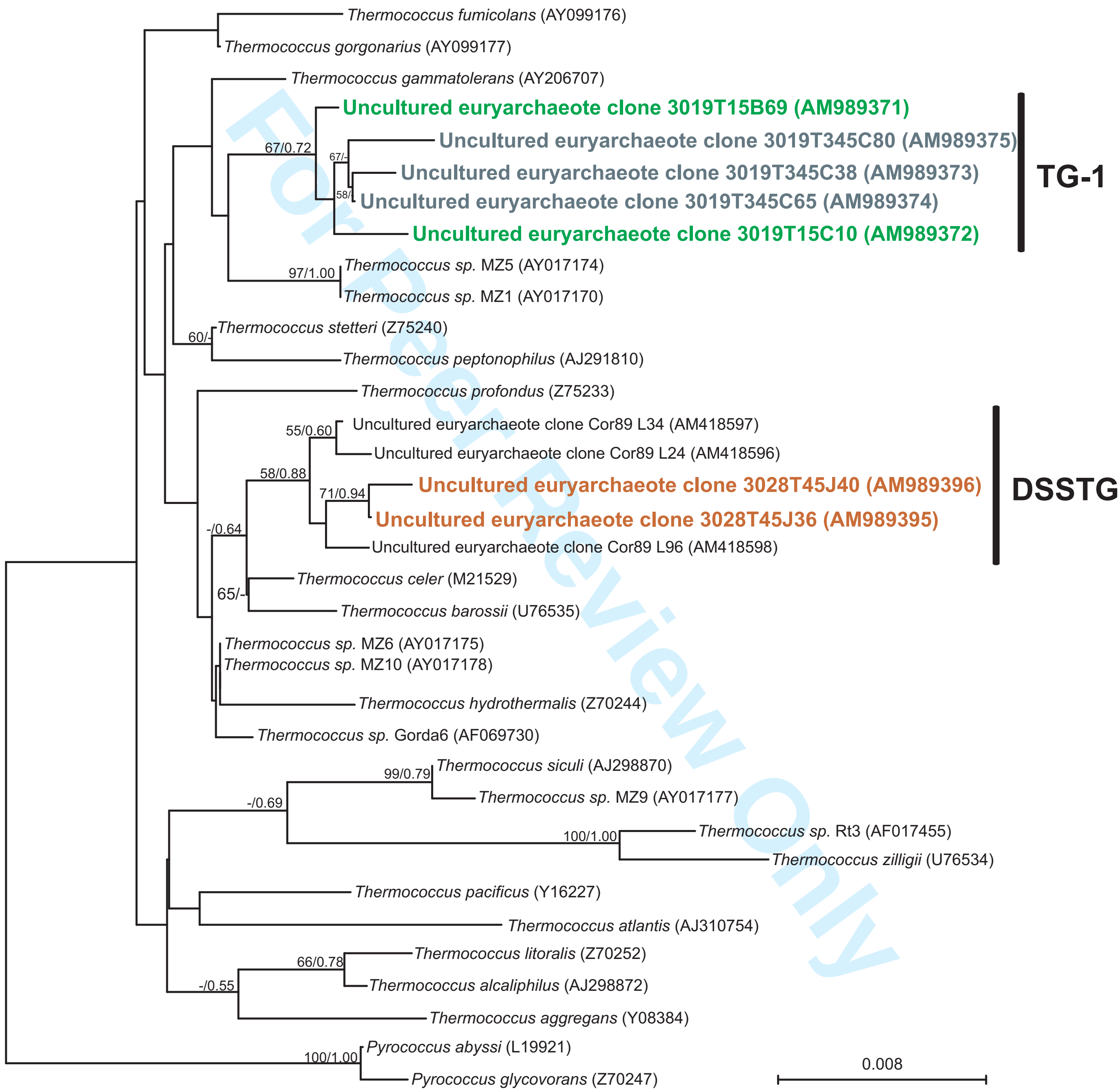
Thermococcus fumicolans (AY099176)
Thermococcus gorgonarius (AY099177)
Thermococcus gammatolerans (AY206707)
Uncultured euryarchaeote clone 3019T15B69 (AM989371)
Uncultured euryarchaeote clone 3019T345C80 (AM989375)
Uncultured euryarchaeote clone 3019T345C38 (AM989373)
Uncultured euryarchaeote clone 3019T345C65 (AM989374)
Uncultured euryarchaeote clone 3019T15C10 (AM989372)
TG-1
67/0.72
67/-
58/
97/1.00
Thermococcus sp. MZ5 (AY017174)
Thermococcus sp. MZ1 (AY017170)
60/-
Thermococcus stetteri (Z75240)
Thermococcus peptonophilus (AJ291810)
Thermococcus profondus (Z75233)
55/0.60
Uncultured euryarchaeote clone Cor89 L34 (AM418597)
Uncultured euryarchaeote clone Cor89 L24 (AM418596)
58/0.88
71/0.94
Uncultured euryarchaeote clone 3028T45J40 (AM989396)
Uncultured euryarchaeote clone 3028T45J36 (AM989395)
Uncultured euryarchaeote clone Cor89 L96 (AM418598)
DSSTG
-/0.64
Thermococcus celer (M21529)
65/-
Thermococcus barossii (U76535)
Thermococcus sp. MZ6 (AY017175)
Thermococcus sp. MZ10 (AY017178)
Thermococcus hydrothermalis (Z70244)
Thermococcus sp. Gorda6 (AF069730)
99/0.79
Thermococcus siculi (AJ298870)
-/0.69
Thermococcus sp. MZ9 (AY017177)
100/1.00
Thermococcus sp. Rt3 (AF017455)
Thermococcus zilligii (U76534)
Thermococcus pacificus (Y16227)
Thermococcus atlantis (AJ310754)
66/0.78
Thermococcus litoralis (Z70252)
-/0.55
Thermococcus alcaliphilus (AJ298872)
Thermococcus aggregans (Y08384)
100/1.00
Pyrococcus abyssi (L19921)
Pyrococcus glycovorans (Z70247)
0.008

Supplementary material

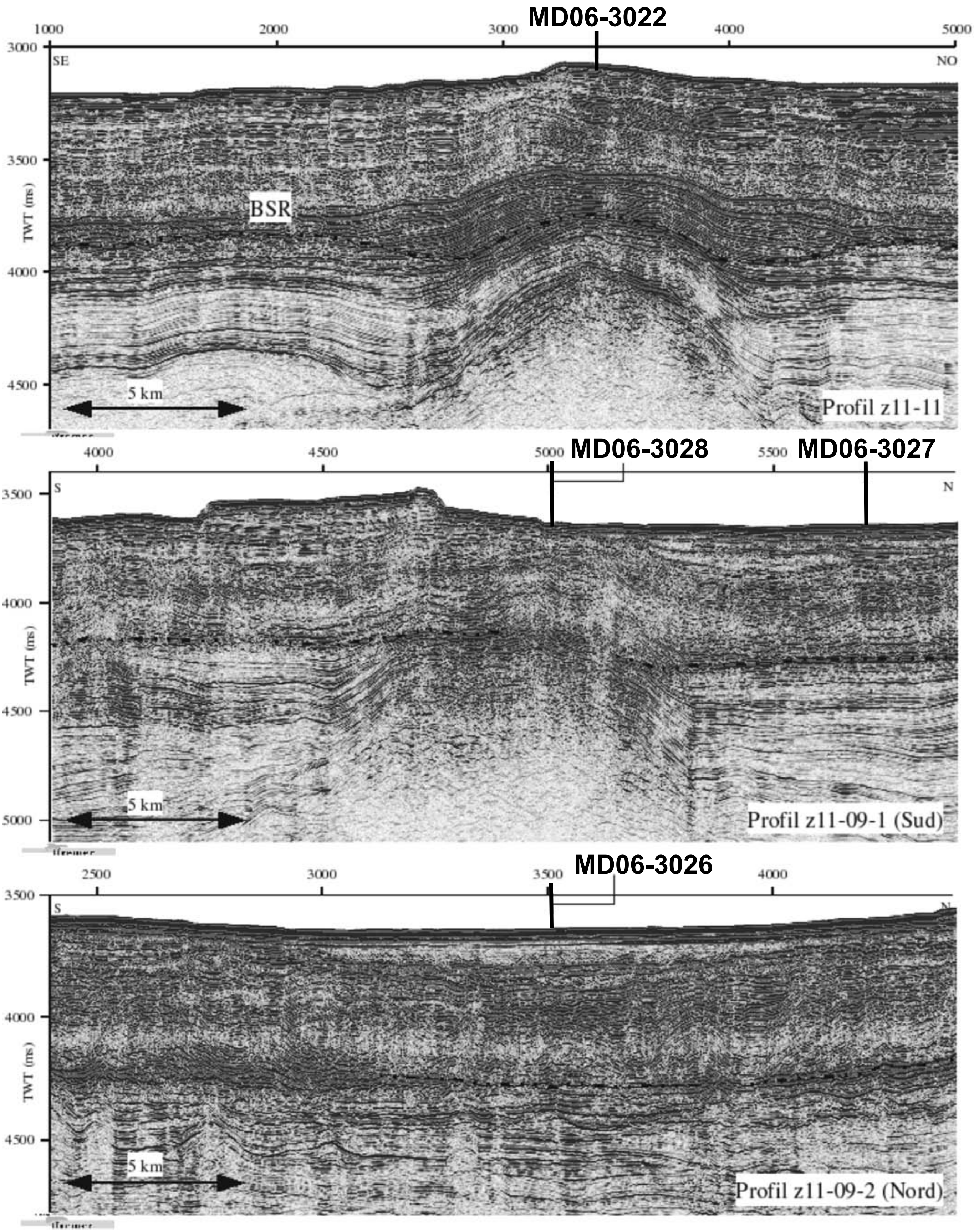

Fig. S1. Seismic profiles of the Fairway Basin on which are located the position of the sites MD06-3022, MD06-3026, MD06-3027 and MD06-3028. Figure modified from Foucher et al. (2006).

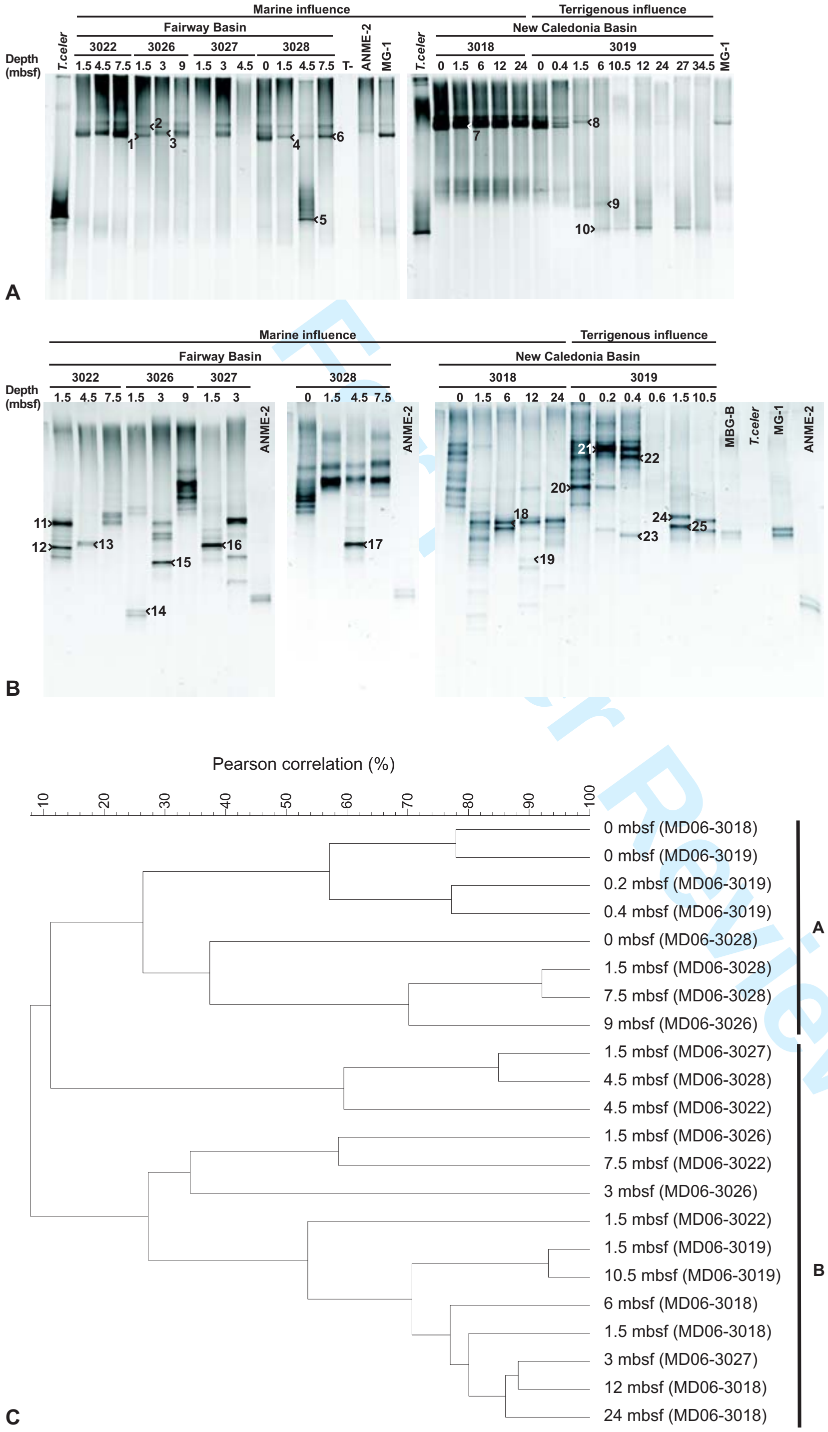

1 ***Thermoplasmatales*** (Unc. arch. clone ZES-79 - EF367516 - 87%)
2 ***Thermoplasmatales*** (Unc. arch. clone ZES-79 - EF367516 - 87%)
3 **MBG-B** (Unc. arch. clone Napoli-2A-38 - AY592501 - 89%)
4 **MG-1** (Unc. crenarch. clone DSA OTU 2 - AJ567637 - 92%)
5 ***Thermococcus*** (*Thermococcus gammatolerans* strain FJ3 - AY206705 - 95%)
6 **MG-1** (Unc. crenarchaeote clone DSA OTU 2 - EF414498 - 92%)
7 ***Thermoplasmatales*** (Unc. arch. clone 3A054 - EF203548 - 86%)
8 **MBG-B** (Unc. crenarch. clone 1a_F4 - AY800203 - 83%)
9 ***Thermococcus*** (*Thermococcus sp.* AT1273 - AJ874326 - 97%)
10 ***Thermococcus*** (*Thermococcus sp.* 23-2 - AY206704 - 99%)
11 ***Thermoplasmatales*** (Unc. arch. clone Amsterdam-1A-25 - AY592254 - 93%)
12 **MG-1** (Unc. arch. clone ZES-238 - EF367675 - 84%)
13 **Unclassified *Euryarchaeota*** (Unc. arch. clone MD2896-1m.2 - DQ984885 - 94%)
14 **Unclassified *Euryarchaeota*** (Unc. arch. clone ZES-79 - EF367516 - 90%)
15 **SAGMEG** (Unc. arch. clone 1H5_D09 - DQ301983 - 93%)
16 **SAGMEG** (Unc. arch. clone MD2896-0.1m.60 - DQ984886 - 93%)
17 **SAGMEG** (Unc. arch. clone MD2896-0.1m.60 - DQ984886 - 92%)
18 **MBG-D** (Unc. euryarch. clone NANK-A120 - AY436522 - 88%)
19 ***Thermoplasmatales*** (Unc. arch. clone Amsterdam-1A-25 - AY592254 - 87%)
20 **MG-1** (Unc. arch. clone 1.8mBB.24 - AY661849 - 96%)
21 **MG-1** (Unc. crenarch. 1.8mBB9 - AJ870326 - 94%)
22 **MG-1** (Unc. crenarch. isolate DGGE gel - DQ137877 - 87%)
23 **MG-1** (Unc. arch. clone 1.8mBB.11 - AY661836 - 93%)
24 **Rice cluster V** (Unc. arch. - AB250587 - 82%)
25 **Rice cluster V** (Unc. arch. - AB250587 - 78%)

Fig. S2. Denaturant gradient gel electrophoresis (DGGE) analysis of archaeal 16S rRNA genes of the cores from the Fairway and New Caledonia Basin sites. The numbered bands were excised and sequenced. The lineage and the sequence similarity of the closest match by BLASTN search are given on the right. (A) PCR products were amplified with the A344fGC-A915r primer set and electrophoresis was performed using a gradient of 40–70% denaturant. (B) PCR products were amplified with the Saf-PARCH 519r primer set and electrophoresis was performed using a gradient of 30–60% denaturant. (C) Cluster analysis of DGGE band patterns. The dendrogram was calculated by Pearson correlation and UPGMA.

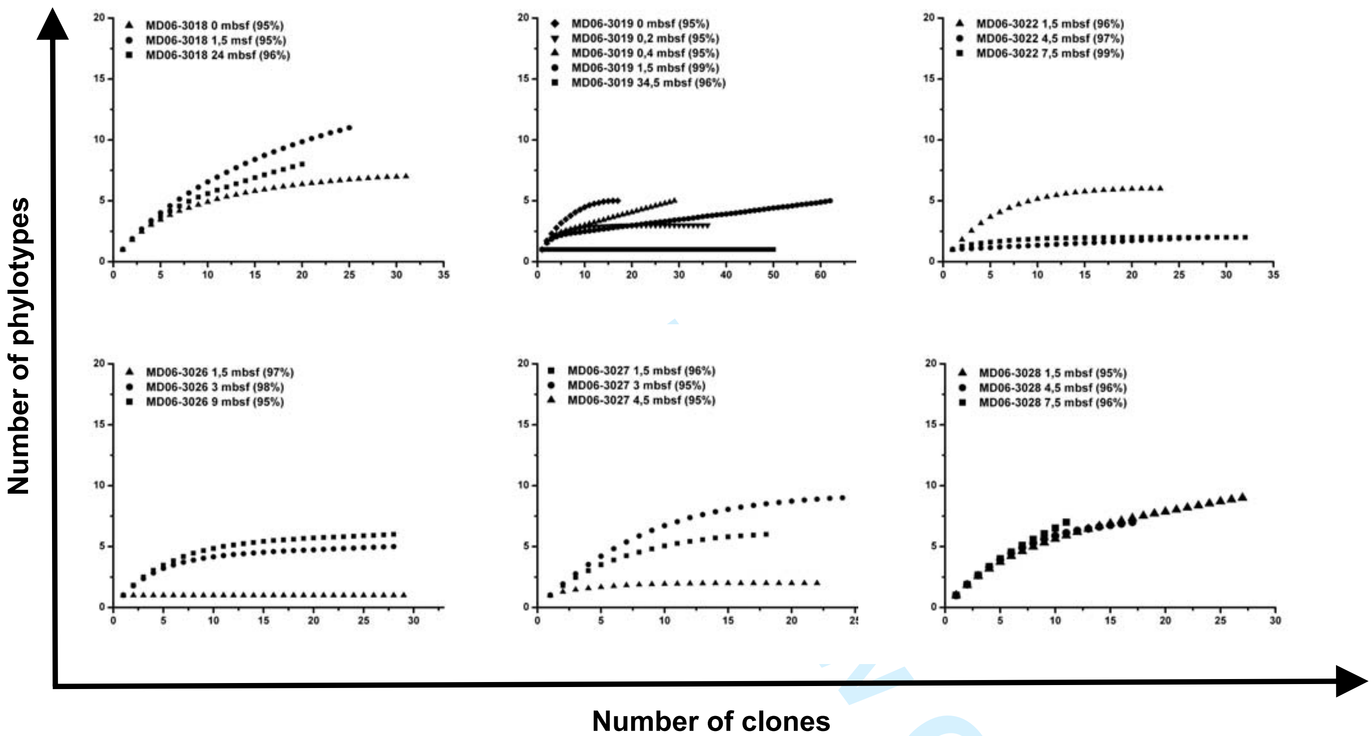

Fig. S3. Rarefaction curves for the 16S rRNA gene clone libraries from the Fairway and New Caledonia Basin sites (Schloss and Handelsman, 2005). The sequence identity levels are represented in brackets.

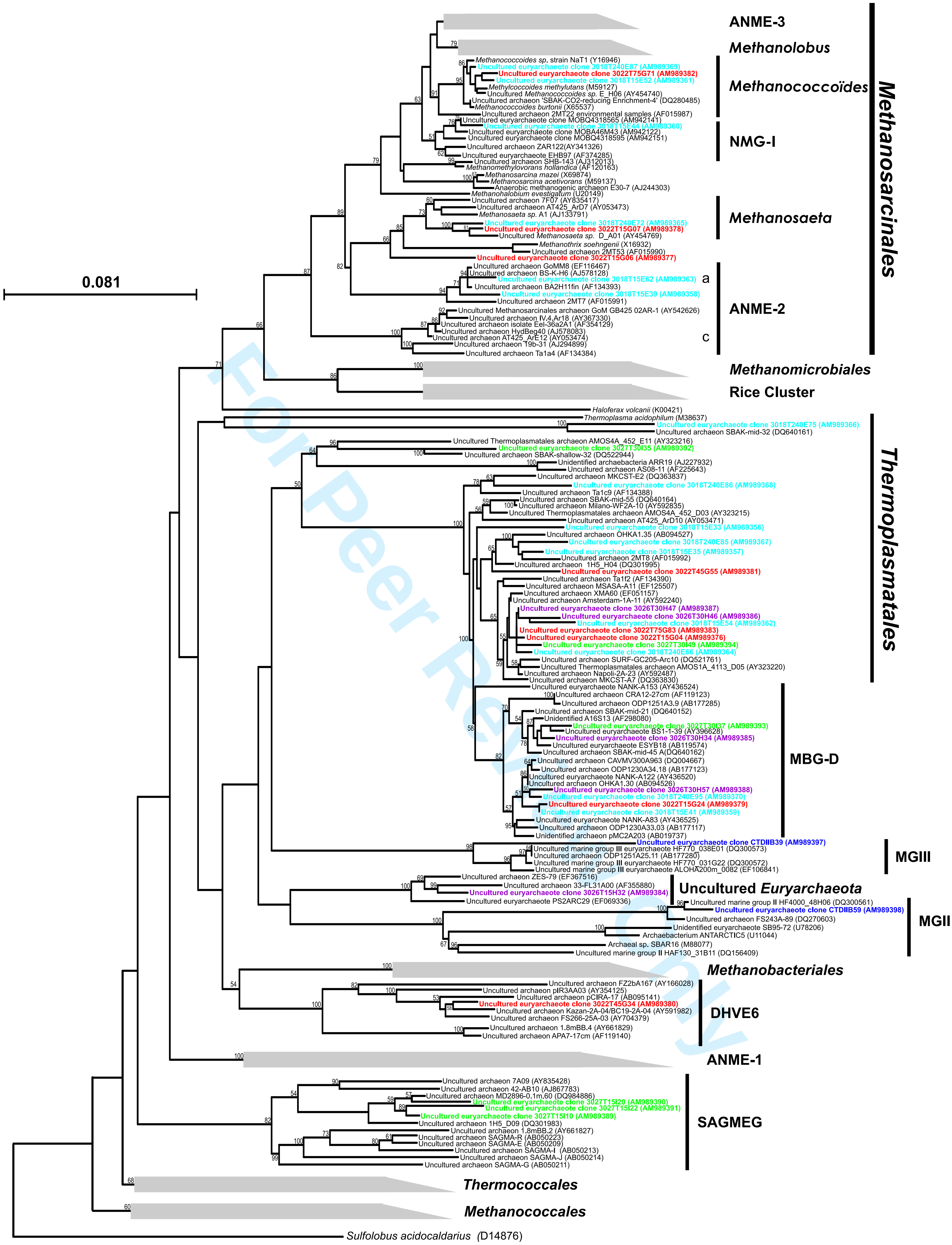

Fig. S4. Phylogenetic tree representing the *Euryarchaeota* 16S rRNA gene, except the *Thermococcales* lineage, sequences DNA- and RNA derived. RNA-derived sequences are underlined. Each phylotype is represented by one sequence with ≥97% similarity grouping. The tree was constructed using the neighbour-joining method with Jukes and Cantor correction. Bootstrap values <50% are not shown. ANME: anaerobic methane oxidizers, NMG-1: Novel *Methanosarcinales* group 1, SAGMEG: South African Gold Mine Euryarchaeotic Group, DHVE6: Deep-Sea Hydrothermal Vent Euryarchaeotal Group 6, MBG-D: Marine Benthic Group D, MG: Marine Groups. Sequences are color-coded according to site location.

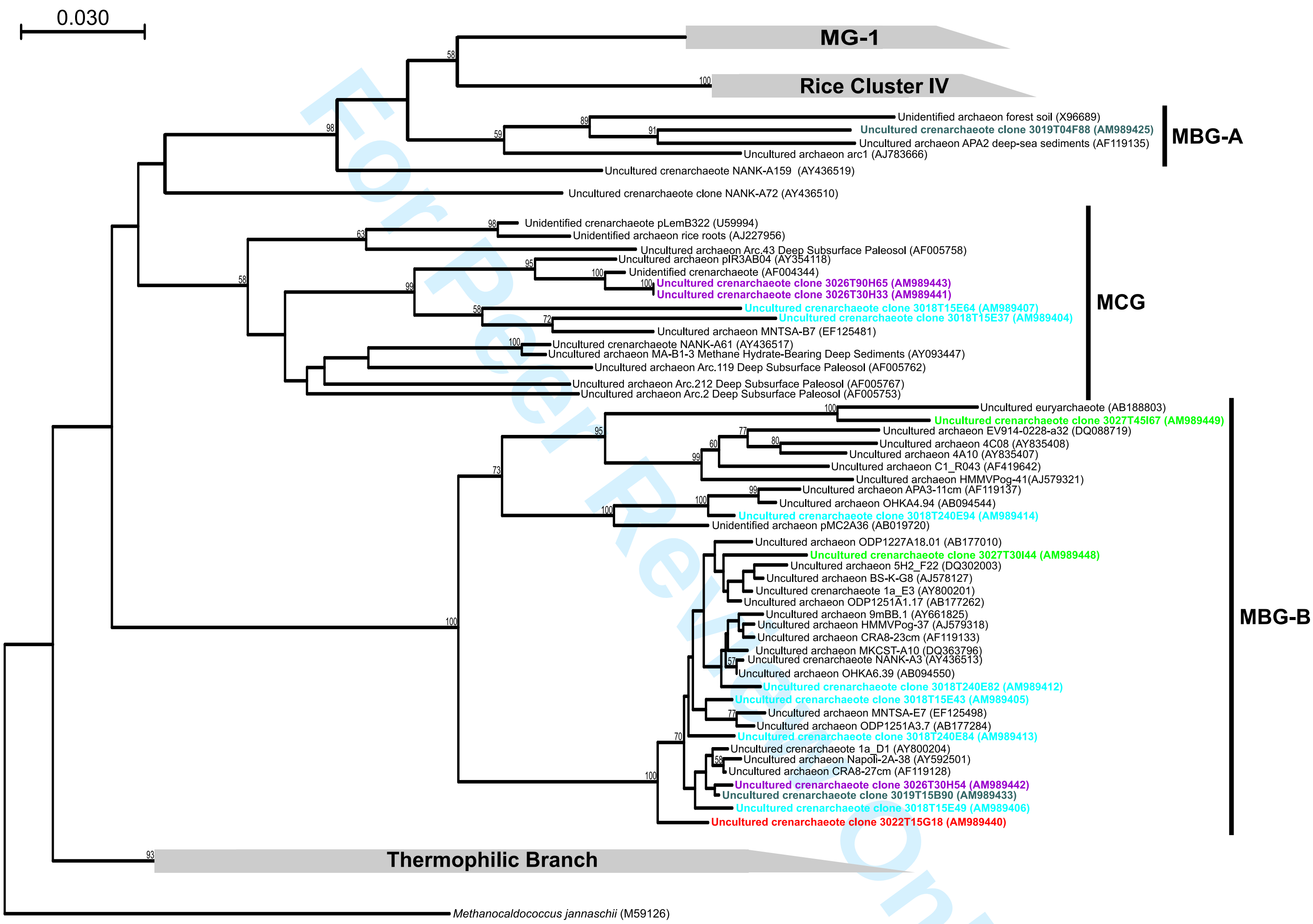

Fig. S5. Phylogenetic tree representing the *Crenarchaeota* 16S rRNA gene sequences, except the MG-1 lineage, DNA- and RNA derived. RNA-derived sequences are underlined. Each phylotype is represented by one sequence with ≥97% similarity grouping. The tree was constructed using the neighbour-joining method with Jukes and Cantor correction. Bootstrap values <50% are not shown. MCG: Miscellaneous Crenarchaeotal Group, MBG-B: Marine Benthic Group B, MBG-A: Marine Benthic Group A. Sequences are color-coded according to site location.

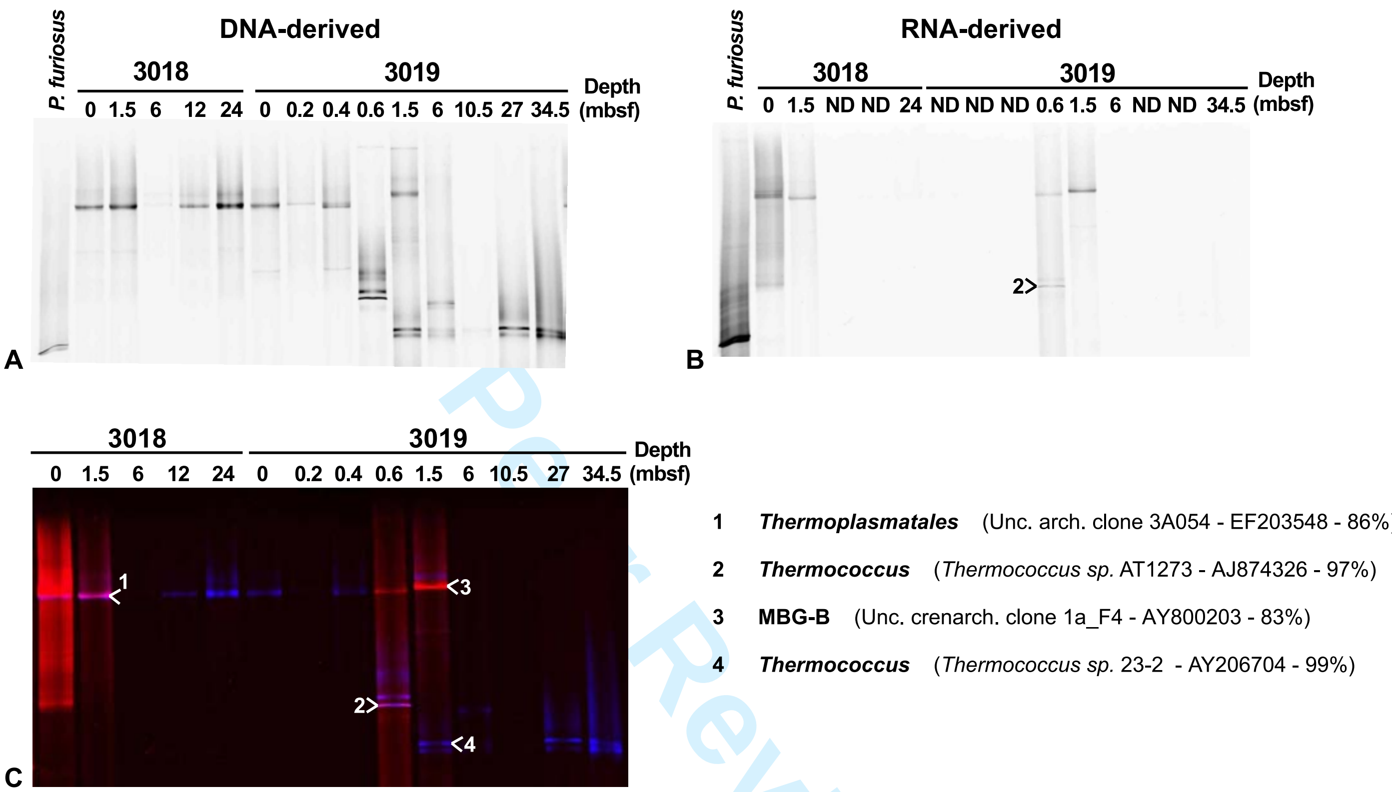

Fig. S6. Co-Migration Denaturant Gradient Gel Electrophoresis (CM-DGGE) analysis of archaeal 16S rRNA genes DNA-derived (blue) and RNA-derived (red) of the cores from MD06-3018 and MD06-3019. The numbered bands were excised and sequenced. The lineage and the sequence similarity of the closest match by BLASTN search are given on the right. PCR products were amplified with the A344fGC-A915r*Cy5 (blue) or A344fGC-A915r*Cy3 (red) primer set and electrophoresis was performed using a gradient of 40–70% denaturant. (A) DNA-derived (A344fGC-A915r*Cy5). (B) RNA-derived (A344fGC-A915r*Cy3). (C) both DNA- and RNA-derived. ND, not determined.

Foucher, J.P., Charlou, J.L., Harmegnies, F., Wirrmann, D., Sémah, A.M., Chaduteau, C., and Roussel, E. (2006) Rapport des travaux de la campagne ZoNéCo 12 : Campagne AUSFAIR/ZoNéCo12 à bord du N/O Marion Dufresne (12 au 26 février 2006). In: IFREMER.

Schloss, P.D., and Handelsman, J. (2005) Introducing DOTUR, a computer program for defining operational taxonomic units and estimating species richness. *Appl Environ Microbiol* **71**: 1501-1506.